Product Level Emission Intensities: Measurement and Application to the Carbon Border Adjustment Mechanism*

Ohyun Kwon Hao Zhao Min Qiang Zhao

August, 2025

Abstract

We estimate product-level emission intensities (PLEI) at the HS 6-digit level for nine pollutants, separating product-specific PLEI from firm-specific factors. Using Chinese firm-level data (2000–2013), we find marked heterogeneity: the top decile of products accounts for nearly 75 percent of emissions but under 4 percent of export volume. A product-level carbon border adjustment mechanism (CBAM) outperforms a sector-level CBAM, delivering larger emission reductions (89 vs. 41 percent) with substantially less trade disruption (1 vs. 5 percent), or achieving the same 41 percent reduction at a far lower carbon price (USD 4 vs. 80 per ton).

JEL classification: F13, F18, Q56

Keywords: International trade and the environment, Product-level emission intensities, Carbon border adjustment mechanism

*Ohyun Kwon: School of Economics, Drexel University LeBow College of Business, ok85@drexel.edu; Hao Zhao: School of Ecology and Environment, Renmin University of China, haozhao@ruc.edu.cn; Min Qiang Zhao: MOE Key Laboratory of Econometrics, the Wang Yanan Institute for Studies in Economics, Xiamen University, kent_zhao@xmu.edu.cn. We thank Lorenzo Caliendo, Davin Chor, Hanming Fang, Paul I. Ko, Giovanni Maggi, Kei-Mu Yi, and Yoto V. Yotov, as well as seminar participants at CUHK, Jinan University, Nanjing University, Peking University, SHUFE, Swarthmore College, UNIST, University of Bari, Zhejiang University, CAERE, KATIS, Midwest Trade and other venues for helpful comments. Hao Zhao acknowledges financial support from the National Natural Science Foundation of China (No. 72303231). Min Qiang Zhao acknowledges financial support from the National Natural Science Foundation of China (No. 71773102).

1 Introduction

How much of the world's emissions can be traced to the production of traded goods? This question is central not only to a range of research questions[1]—such as how firms in advanced economies reduce domestic emissions through offshoring—but also to the design of cross-border climate policy instruments, most notably the European Union's (EU) Carbon Border Adjustment Mechanism (CBAM).

A common approach to quantifying emissions embodied in trade is to multiply *sector*-level emission intensities by corresponding trade volumes. While widely adopted, this method obscures considerable *product*-level heterogeneity and may introduce aggregation bias (Levinson, 2023). This paper develops a new methodology for estimating product-level emission intensities (PLEI) by combining firm-level emissions data with firm-product-level output. The approach yields highly granular measures of embodied emissions at Harmonized System (HS) 6-digit level, enabling a more precise understanding of the environmental consequences of international trade.

The contributions of this paper are threefold. First, we develop a novel algorithm for estimating PLEI that iteratively reconciles firm-level emissions allocations across products within a firm with aggregate-level emission intensity measures, thereby ensuring *micro-macro consistency*. In contrast to our approach, existing methods typically allocate a firm's emissions across products in proportion to output shares, which violates this consistency.[2]

Beyond ensuring micro-macro consistency, our algorithm offers several advantages: (i) it produces PLEI estimates at a highly disaggregated level (HS 6-digit); (ii) it is consistent with heterogeneous multi-product firm frameworks, such as Bernard et al. (2010) and

[1]For instance, Zhang et al. (2017) estimate that western European and U.S. consumption—through trade—contributed to over 108,600 premature deaths in China due to elevated PM 2.5 levels in export production. Other relevant research questions include, but are not limited to, whether pollution offshoring leads to a net increase in global emissions (Duan et al., 2021), and whether the Kyoto Protocol induces carbon leakage (Aichele and Felbermayr, 2015).

[2]Specifically, allocating emissions based on output shares is valid only when all products exhibit identical emission intensities—an assumption that is inconsistent with highly heterogeneous PLEI.

Shapiro and Walker (2018), and enables the decomposition of firm-product emission intensity into a product-level component (PLEI) and a firm-time-specific inefficiency term; and (iii) it is broadly applicable to any country with data on firm-level emissions and firm-product-level output.

To describe the algorithm concisely, we begin with an initial guess for PLEI, which is used to allocate each firm's total emissions across its products. These firm-product-level emissions are then aggregated across all firms and divided by the corresponding aggregate product output to update the PLEI estimates. The procedure iterates until convergence. Monte Carlo simulations confirm the algorithm's robustness to initial values, modeling assumptions, and measurement error, and demonstrate its superiority over alternative methods.

Second, we document new stylized facts on PLEI using Chinese firm-level emissions data from 2000 to 2013. Specifically: (i) PLEI exhibit substantial heterogeneity across products; (ii) the top 10% most emission-intensive products account for nearly 75% of total emissions but only 4% of export volume; (iii) aggregating to broader product classifications significantly understates this heterogeneity; and (iv) China did not shift toward more emission-intensive exports following WTO accession.

Third, we use the estimated PLEI to evaluate counterfactual CBAM regimes. We show that, relative to a benchmark sector-level CBAM, a product-level CBAM can (i) achieve a substantially larger reduction in emissions (89% vs. 41%) at the same carbon price of USD 80 per ton, or (ii) attain the same 41% reduction at a much lower price (USD 4 vs. 80 per ton). In both cases, the product-level CBAM results in considerably smaller losses in trade volume and real income.

The methodology and findings of this paper have direct implications for research and policy. By introducing a new approach to estimating granular PLEI, our framework enables more accurate empirical analysis and supports the design of more cost-effective climate policies.

Related Literature.

Shapiro and Walker (2018) use U.S. Census data to estimate PLEI for 1,440 products, representing, to the best of our knowledge, the most detailed effort to date. However, their method allocates firm-level emissions to products in proportion to output values—an approach equivalent to assuming uniform emission intensities across products, and therefore inconsistent with the substantial heterogeneity we document in PLEI. Our study introduces an iterative algorithm that ensures micro-macro consistency between firm-product-level emission allocations and economy-wide PLEI estimates. Furthermore, leveraging customs data enables us to estimate PLEI for a substantially more granular spectrum of approximately 4,500 products.[3]

In a recent study, Shapiro (2021) computes industry-level CO_2 intensities using the Exiobase global input-output table across 163 industries. A notable difference with our approach is that our PLEI calculations encompass emissions linked to domestic intermediate inputs and value-added, whereas Shapiro's metrics additionally incorporate emissions from imported intermediate inputs. Put differently, our PLEI framework quantifies emissions related to China's *value-added* in global value chain, while Shapiro's methodology accounts for emissions in China's *gross exports*. It is important to note that neither approach is inherently superior and their relevance depends on the context. For example, in our CBAM application, we argue that tariffs should be based on China's value-added emissions, because imported intermediate inputs—potentially from regions such as Europe where carbon is already priced—should not be double-counted.[4]

Our research contributes to the growing literature on environmental emissions in international trade (Ederington et al., 2005; Frankel, 2009; Cherniwchan, 2017; Larch and Wanner, 2017; Tanaka et al., 2022; Choi et al., 2025).[5] This literature includes studies es-

[3]Firm-product-level emissions data are available in a few countries but remain uncommon (e.g., Barrows and Ollivier (2018)). Our methodology requires only firm-level emissions data, making it readily scalable to a broader set of countries.

[4]Similarly, when evaluating China's global CO_2 contribution, it is more appropriate to focus on emissions associated with China's value-added rather than gross exports.

[5]For comprehensive reviews, see Copeland and Taylor (2004), Cherniwchan et al. (2017), and Copeland

timating emissions embodied in trade flows—such as CO_2 emissions in China's value-added exports (Dietzenbacher et al., 2012), carbon leakage after the Kyoto Protocol (Aichele and Felbermayr, 2015), and the welfare impacts of trade liberalization (Shapiro, 2016). Our PLEI measures offer new empirical tools for this literature that reduce aggregation bias and enable more precise, product-level assessments of emissions embodied in trade.

Our paper also contributes to the looming literature on CBAM.[6] Specifically, a number of studies have explored the design and the economic impacts of CBAM (Böhringer et al., 2014; Keen and Kotsogiannis, 2014; Böhringer et al., 2016; Balistreri et al., 2019; Bellora and Fontagné, 2023; Kortum and Weisbach, 2023; Farrokhi and Lashkaripour, 2025). The novel insight from our paper is that CBAM's implementation efficiency can be improved substantially if product-level information can be taken into account.[7]

The paper proceeds as follows. Section 2 describes the data and methodology for estimating PLEI. Section 3 presents new stylized facts on PLEI. Section 4 evaluates the implications of PLEI for CBAM policy design. The last section concludes.

2 Product-Level Emission Intensities

This section outlines the primary data sources at the core of our analysis and presents our novel approach to compute PLEI.

2.1 Data Source

The primary dataset for our study is China's Environmental Statistical Database (CESD), encompassing firm-level panel data pertaining to emissions. In each year, leading enterprises responsible for 85% of emissions within each county submit detailed reports

et al. (2022).

[6]See Fontagné and Schubert (2023) for a comprehensive review of the CBAM literature. Relatedly, Nordhaus (2015) proposes the idea of a climate club where domestic carbon policies can be coordinated. Staiger (2022) discusses integrating climate change into the existing world trade system.

[7]Emissions associated with the transportation of traded goods (Klotz and Sharma, 2023; Copeland et al., 2022), while important, are beyond the scope of this paper.

regarding their emission metrics, energy consumption, and abatement measures to the Ministry of Ecology and Environment. Within this dataset, our primary focus lies on industrial water utilization and emissions, including COD, SO_2, NO_x, CO_2, industrial exhaust, ammoniacal nitrogen, soot, and dust.[8] To merge CESD with other datasets, we use information such as the firm's name, organizational code, postal code, and administrative location code. The CESD dataset is widely used in environmental studies in China (Liu et al., 2017; Fan et al., 2025), and its rigorous data collection protocol mitigates incentives for firms to misrepresent emission records (He et al., 2020). As for the data quality, studies have cross-validated the dataset with the U.S. satellite data for SO_2 (Rodrigue et al., 2022a).

The second dataset is the Annual Survey of Industry Enterprises (ASIE) for Chinese firms. The ASIE dataset covers state-owned enterprises and private firms with annual sales above 5 million RMB (20 million RMB since 2011). It includes key firm-level information such as industry classification and total sales. The CESD and the ASIE data can be merged together based on firms' organization code and company name. Kwon et al. (2023) show that this matching process successfully captures over 75% of the output reported in the CESD.

To identify the HS 6-digit products exported by firms, we further merge our firm-level dataset with Chinese customs data using firm identifiers, following Roberts et al. (2018) and Yu (2015). This linkage allows us to observe export values by product at the firm-year level. We compute domestic sales by subtracting total exports from total sales, which in turn allows us to estimate emission intensities associated with domestic output.

Following Levinson (2009), we compute both direct and total emission intensities. *Direct* emission intensity is defined as emissions generated in the final production stage normalized by total production value. *Total* emission intensity incorporates emissions along

[8] CO_2 emissions primarily result from burning fossil fuels. The CESD dataset details each firm's use of coal, natural gas, and oil. To estimate carbon emissions, we multiply the consumption of each type of energy by its corresponding carbon emission factor, as determined by Guidelines for Provincial Greenhouse Gas Inventories published by National Development and Reform Commission of China.

the entire domestic value chain. To construct this measure, we use China's input-output table from EORA, a widely used source in international trade research. Finally, we rely on BACI (Gaulier and Zignago, 2010) trade data to compare China's trade flows with the rest of the world.[9]

2.2 Methodology, Validation and PLEI Estimates

In most datasets, firms do not report emissions separately for each product they produce. Accordingly, we develop a novel method for allocating emissions across products that aligns with standard assumptions in the literature while ensuring internal consistency.

Our conceptual framework assumes that a firm's emission intensity for a given product can be decomposed into two components. The first is the economy-wide emission intensity of product h, denoted ζ_h ($\zeta_h \geq 0$), which reflects the inherent characteristics of the production process and is common across firms. For instance, producing steel generates more CO_2 emissions per unit of value than producing smartphones. We introduce the parameter ζ_h to capture this product-level variation, which we refer to as PLEI.

The second component is a firm-specific *inefficiency* parameter, denoted λ_i ($\lambda_i > 0$), which captures variation in emissions across firms producing the same product. This reflects differences in environmental performance and is often linked to variation in productivity (Shapiro and Walker, 2018; Forslid et al., 2018) and to the discriminatory enforcement of environmental regulations (Fan et al., 2025; He et al., 2020).

We model firm-product-level emission intensity as the product of a product-specific baseline and a firm-specific inefficiency term:

$$\zeta_{hi} = \zeta_h \cdot \lambda_i. \tag{1}$$

For instance, a firm with $\lambda_i = 1.2$ emits 20% more CO_2 per unit of output than the product-level benchmark ζ_h. A few discussions regarding equation (1) are in order.

[9] Additional datasets employed for the CBAM application in Section 4 are detailed in Appendix G.2.

First, in our theoretical appendix (Appendix A), we develop a multi-product firm model in the spirit of Bernard et al. (2011). We formally derive equation (1), showing that ζ_h reflects a product's emission elasticity, the average productivity of its producers, and the average stringency of environmental policy they face. In contrast, λ_i captures firm-specific deviations driven by idiosyncratic productivity or firm-level regulatory enforcement.

Second, equation (1) assumes that the firm-specific inefficiency term λ_i applies uniformly across all products in a firm's product mix. This assumption is empirically plausible: 81.40% of firms in our sample produce only a single product.[10] For multi-product firms, our specification is consistent with the theoretical foundations in Bernard et al. (2011) and Barrows and Ollivier (2018), which posit the existence of a "core productivity" parameter that uniformly influences all product lines.

In Appendix A, we formalize this notion. We show that under a model in which firms draw product-specific technologies in addition to a core productivity, the expected firm-product emission intensity satisfies:

$$\mathbb{E}\left[\zeta_{hi}\right] = \zeta_h \cdot \lambda_i.$$

That is, the expected firm-product emission intensity (averaged across many firms) can be expressed as in equation (1). Any product-level deviation from equation (1) can be interpreted as white noise around the conditional mean, and becomes negligible as the number of firms increases. Our Monte Carlo simulations in Section 2.2.1 confirm that such variation has minimal impact on the algorithm's performance, owing to the large number of firms in the data.[11] In sum, the prevalence of single-product firms, support from theoretical foundations, and the robustness of our estimation procedure together

[10] As we do not observe the specific products firms sell domestically, we aggregate all domestic sales to a broad product category defined by the firm's 4-digit CIC industry classification. Accordingly, a firm is considered "single-product" if it either sells exclusively in the domestic market or exports only one HS 6-digit product with no domestic sales.

[11] Firm-level deviations from equation (1) may be either correlated or uncorrelated across firms. If correlated, estimation of ζ_h absorbs this systematic component. If uncorrelated, these deviations act as classical measurement error, which vanishes as the number of firms producing product h increases.

justify the use of equation (1) in constructing PLEI.

Third, the panel structure of our dataset allows for time-varying firm inefficiency parameters, λ_{it}, enabling us to capture temporal fluctuations in productivity or abatement practices. In this setting, ζ_h represents the long-run average PLEI for product h over the period 2000–2013, reflecting time-invariant product characteristics. Temporal improvements in production cleanliness are absorbed by declines in firm-specific λ_{it}.

Finally, emissions associated with domestic sales play a critical role, as they affect the allocation of emissions to export activities. For domestic transactions, we estimate PLEI at the 4-digit CIC (Chinese Industrial Classification) level, covering 603 sectoral categories in our dataset. In what follows, the index set h includes both HS 6-digit export products and 4-digit CIC domestic sectors.

Our PLEI calculation proceeds iteratively as follows:

1. Initialize a guess for the vector of emission intensities, ζ_h.
2. Using equation (1), compute firm i's emissions attributable to product h as:
$$z_{hi} = z_i \frac{\frac{y_{hi}}{y_i}\frac{z_{hi}}{y_{hi}}}{\sum_{h'}\frac{y_{h'i}}{y_i}\frac{z_{h'i}}{y_{h'i}}} = z_i \frac{s_{hi}\zeta_h\lambda_{it}}{\sum_{h'} s_{h'i}\zeta_{h'}\lambda_{it}} = z_i \frac{s_{hi}\zeta_h}{\sum_{h'} s_{h'i}\zeta_{h'}}, \quad (2)$$
where z_i is total emission from firm i, y_{hi} is the firm's production of product h, y_i is the firm's total production, s_{hi} $(\equiv y_{hi}/y_i)$ is the production share of the product. Note that the first equal sign in (2) simply reflects an identity, the second equal sign applies equation (1), and the last one simply cancels out λ_{it}. As such, given firm-level emissions z_i, product shares s_{hi}, and the initial guess for ζ_h, equation (2) yields firm-product emissions z_{hi}.
3. The economy-wide total pollution associated with product h is $Z_h = \sum_i z_{hi}$. We can then update the guess of emission intensities by
$$\zeta_h' = \frac{Z_h}{Y_h} \quad (3)$$
where $Y_h(\equiv \sum_i y_{hi})$ is the economy-wide total production of product h.
4. If ζ_h' are sufficiently close to ζ_h, the iteration process stops; otherwise, ζ_h' replace ζ_h for the next round of iteration.

Our algorithm is particularly useful in settings where product-level emissions within a firm are unobserved—a common feature in firm-level emissions datasets (e.g., National Emissions Inventory). A simplified version of this approach appears in Shapiro and Walker (2018), where firm-level emissions are allocated to products in proportion to output shares. This yields the expression $z_{hi} = z_i s_{hi} / \sum_{h'} s_{h'i}$, which is a special case of equation (2) under the assumption that ζ_h is constant across products.[12]

In contrast, our iterative algorithm ensures consistency at both levels: emissions are allocated across products within a firm using the estimated PLEI (micro consistency, equation (2)), and PLEI itself is defined as the economy-wide average emission intensity (macro consistency, equation (3)). Together, these features achieve the micro-macro consistency highlighted in the Introduction.

Under our framework, the parameter λ_{it} captures firm-year-specific inefficiency—reflecting variation in productivity (Shapiro and Walker, 2018), emissions abatement (Forslid et al., 2018; Kwon et al., 2023), market power (Rodrigue et al., 2022a), and regulatory stringency (He et al., 2020). A useful feature of our algorithm is that λ_{it} cancels out in equation (2), allowing us to accommodate firm-year heterogeneity without requiring knowledge of the exact λ_{it} values when estimating ζ_h.[13]

For our algorithm to deliver reliable results, it is essential that each product is produced by a sufficiently large number of firms, thereby neutralizing the influence of firm-specific variations. To this end, we exclude the products with fewer than 11 firm-year observations.[14] Our refined sample comprises 5,144 product categories, segmented into 603 domestic industries and 4,541 HS 6-digit products. This dataset encompasses 666,213

[12] Applying this output-share-based method to our data yields PLEI estimates with relatively low correlation with our preferred estimates, ranging between 0.1 and 0.3.

[13] Although λ_{it} is not estimated during the iteration procedure, it can be inferred after convergence of ζ_h. We focus on PLEI but provide a brief discussion of λ_{it} in Section 2.4.3, where we show that its distribution is consistent with empirical patterns: it declines over time and is higher among low-productivity firms and state-owned firms.

[14] Specifically, we first drop HS products with fewer than 11 firm-year observations. Next, we compute CIC-level domestic output as total output minus export values, effectively reallocating the dropped HS products to domestic production. Finally, we drop CIC industries with fewer than 11 firm-year observations.

firm-year observations with minor deviations across pollutants due to data availability. On average, each product has 440 firm-year observations, with a median of 140. Given the large number of observations associated with each product, we contend that this allows for a precise estimation of the PLEI common to all firms.

2.2.1 Monte Carlo Simulations

We use Monte Carlo simulations to assess the performance of our algorithm across a range of scenarios. A brief description of the data-generating process (DGP) and main findings are presented here, with full details provided in Appendix B.

The DGP preserves three key empirical features: the distribution of ζ_h estimates, the firm-to-product ratio, and the distribution of product counts across firms. To examine robustness to data noise, we introduce a uniformly distributed multiplicative measurement error ranging from 70% to 130%. We also consider a setting in which the inefficiency term λ_{hi} may vary across products within a firm. All results are based on 500 independent simulations.

Key findings from the Monte Carlo simulations are as follows. First, our iterative procedure recovers the "true" (presumed) ζ_h values with high precision. Across 500 simulations, both the median and mean pairwise correlations between the estimated and true ζ_h exceed 0.998, with standard deviations below 0.002. These results demonstrate that the algorithm is highly robust to the substantial measurement error introduced in the DGP.

Second, even when the DGP departs from our assumption—allowing the inefficiency term λ_{hi} to vary across products within firms—our algorithm continues to recover the ζ_h values with high accuracy. The median and mean correlations remain above 0.998, though the standard deviation of the correlation coefficients increases slightly to 0.003. This strong performance is partly explained by the structure of the data: 81.40% of firms produce a single product, and an additional 7.25% produce only two or three. As a result, a single firm-level inefficiency term λ_i can parsimoniously capture cross-firm variation in

PLEI, even in the presence of firm-product-level idiosyncrasies.

As a supplementary analysis, we also estimate ζ_h using ordinary least squares (OLS) using the following specification:

$$z_i = \sum_h y_{hi}\zeta_h + e_i,$$

where z_i denotes firm-level emissions, y_{hi} is firm-product output, and e_i is the error term. The OLS approach paradoxically yields negative ζ_h estimates for approximately half of the products. Moreover, even when restricted to products with positive estimates, the correlation with the "true" ζ_h is lower and exhibits substantially greater dispersion compared to our iterative method. Overall, the Monte Carlo results underscore the reliability and robustness of our iterative approach.

2.2.2 Total Domestic Emission Intensities

The output from our iterative algorithm is typically referred to as *direct* emission intensity, capturing emissions associated with the final production process. This stands in contrast to *total* emission intensities, which encompass the cumulative emissions across the entire value chain in domestic production.[15]

To derive total emission intensities, we follow the conventional method. Consider $\mathbf{C}$ as an N-by-N matrix of direct requirement coefficients. Each element, denoted by c_{ij}, specifies the monetary value of the input from industry i (row) requisite for generating a dollar's output in industry j (column). The vectors $\mathbf{x}$ and $\mathbf{y}$ respectively represent the aggregate output and the total final demand of industry i. With this construction, the relationship can be expressed as:

$$\mathbf{x} = \mathbf{C}\mathbf{x} + \mathbf{y}. \tag{4}$$

[15] Studies such as Levinson (2009), Lyubich et al. (2018), and Shapiro (2021) have employed similar methods for computing total emission intensities. Notably, both Levinson (2009) and Lyubich et al. (2018) limit their considerations to domestic intermediate inputs. In contrast, Shapiro (2021) extends this by accounting for emissions embedded in imported intermediate components. We align with the former methodology, primarily because direct emission intensities at the HS 6-digit level for countries other than China are not yet available. Moreover, total domestic emission intensity is more relevant for our CBAM application.

This expression demonstrates that the industrial output, represented by $\mathbf{x}$, is either assimilated as intermediate input, denoted by $\mathbf{Cx}$, or used as final goods, represented by $\mathbf{y}$.

Rearranging terms, we derive: $\mathbf{x} = [\mathbf{I} - \mathbf{C}]^{-1}\mathbf{y}$, where the matrix $[\mathbf{I} - \mathbf{C}]^{-1} \equiv \mathbf{T}$ is referred to as the Leontief total requirements matrix (Leontief, 1970). In this matrix, each element, represented by t_{ij} in $\mathbf{T}$, quantifies the monetary output of industry i required for the final production in industry j. Let $\boldsymbol{\zeta}$ and $\tilde{\boldsymbol{\zeta}}$ denote direct and total emission intensities, respectively. The relationship $\tilde{\boldsymbol{\zeta}}'\mathbf{y} = \boldsymbol{\zeta}'\mathbf{x}$ holds, wherein both sides of the equation correspond to the aggregate emissions in the economy. Consequently, the total pollution coefficients, $\tilde{\boldsymbol{\zeta}}$, can be expressed as:

$$\tilde{\boldsymbol{\zeta}}' = \boldsymbol{\zeta}'\mathbf{T}. \tag{5}$$

To calculate the Leontif matrix, we employ the EORA dataset, which provides an input-output table encompassing 87 industries in China: 6 agricultural, 6 mining, 72 manufacturing, and 3 utility sectors.[16] Since this table aggregates products more broadly than the PLEI, we make two key assumptions. First, we assume that all products within an individual EORA industry demand the same input bundle per unit of output. Additionally, we assume that input supplies within an EORA industry are distributed across corresponding HS 6-digit products and 4-digit CIC sectors in proportion to each product's or sector's output share.

Figure 1 plots direct emission intensities (horizontal axis) against total emission intensities (vertical axis) for CO_2, which has received considerable attention in the context of global warming.[17] Several patterns are noteworthy. First, total emission intensities consistently exceed their direct counterparts, as they incorporate emissions from both domestic intermediate inputs and final production. Second, the gap is more pronounced for

[16]While the EORA input-output table also includes service industries, they are excluded from our analysis since the firms in our dataset do not belong to these sectors.

[17]Throughout the main text, we focus on CO_2 emissions. Results for other pollutants are similar and reported in Appendix F.

Figure 1: Direct vs. Total Emission Intensities (CO_2)

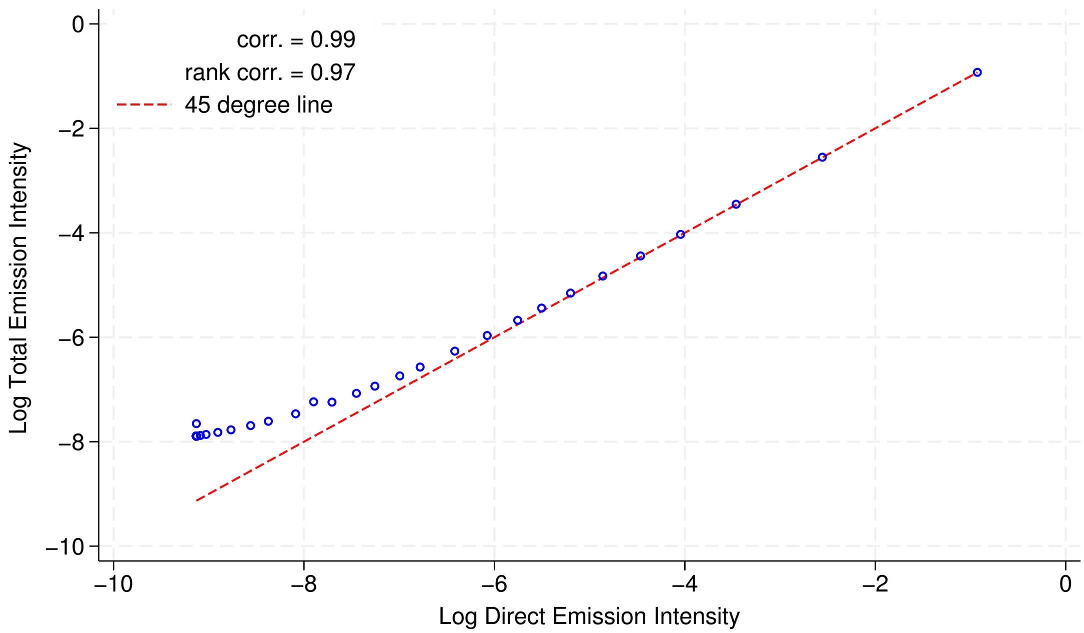

Notes: This figure compare the logarithmic values of direct and total emission intensities for CO_2. We add the smallest value of total emission intensities to all values before log transformation to account for zero emission intensities. For exposition, we sample one HS 6-digit product from each of 100 percentile values of direct emission intensities and display it as a dot. The dots presented in the figure appear to be less than 100 as many dots overlap each other toward zero direct emission intensities. The displayed correlations are derived from the full distribution of emission intensities rather than the 100 displayed dots. Similar figures for other pollutants are presented in Appendix Figures F.3 and F.4.

products with low direct emission intensity: even small quantities of dirty intermediate inputs can substantially elevate total emissions. By contrast, products with high direct intensity show only modest increases in total measures, as their intermediates are relatively cleaner. Both correlation and rank-correlation between the two measures exceed 0.97.

Figure 1 thus shows that relying solely on direct emission intensities may underestimate total emissions, particularly when the final production stage is relatively clean. However, this compression in the distribution of PLEI does not significantly affect product rankings, and the conclusions from our subsequent analysis are robust to the choice between direct and total emission intensities.

2.3 Validation

We employ two main strategies to validate our PLEI estimates. First, we assess whether products identified as emission-intensive align with established expectations regarding the sources of industrial emissions. This qualitative evaluation provides face validity for our measures. Second, we aggregate the PLEI estimates to the industry level and compare them with emission intensities derived from external datasets, offering a quantitative benchmark for validation.

2.3.1 Top Emission Intensive Products

In Tables 1 and 2, we enumerate the top emission-intensive product groups, as characterized by their total PLEI levels. We focus our attention primarily on CO_2 and COD, with corresponding tables for other pollutants relegated to Appendix F. Each table showcases the six most emission-intensive HS 2-digit product groups, alongside the three leading emission-intensive HS 6-digit products within each category.

Both tables align closely with conventional expectations. Table 1, for instance, identifies the glass, cement, inorganic chemicals, and metal industries as major CO_2 emitters, consistent with their reliance on energy-intensive processes and coal combustion.

These sectors are likewise recognized by the European Union as CO_2-intensive industries.[18] Similarly, Table 2 highlights the chemical, paper, textile, and leather industries as significant contributors to COD emissions, which is expected given their intensive chemical use and high wastewater output. We view the intuitive industry patterns shown in both tables—as well as in additional pollutant-specific tables in Appendix F—as supporting evidence that our PLEI estimates capture the intrinsic emission characteristics of production processes.

2.3.2 Industry-Level External Validation

A viable strategy for externally validating our PLEI estimates involves aggregating them to the industry level and comparing the resulting emission intensities with those derived from alternative data sources.[19] We present full details in Appendix C and summarize the key findings here. Across several pollutants, the aggregated PLEI measures exhibit mean correlation coefficients of 0.79 with the Chinese Statistical Yearbook, 0.48 with EXIOBASE, and 0.46 with EORA. These results lend support to the validity of our PLEI estimates, indicating that—when aggregated—they closely track industry-level emission intensities reported in widely used datasets.

[18]See European Parliament resolution on the Carbon Border Adjustment Mechanism: https://www.europarl.europa.eu/doceo/document/TA-9-2021-0071_EN.pdf (accessed on July 28, 2025).

[19]While Shapiro and Walker (2018) compute product-level emission intensities for 1,440 five-digit SIC industries using U.S. Census data, data access restrictions prevent direct comparison with their estimates.

Table 1: Top CO_2-intensive Products

HS Code	Description
700000	**Glass and glassware**
700239	Glass; unworked, in tubes, other than of glass having a linear coefficient of expansion n...
701391	Glassware; n.e.c. in heading no. 7013, of lead crystal
700210	Glass; unworked, in balls (other than microspheres of heading no. 7018)
250000	**Plastering materials, lime and cement**
250610	Quartz; other than natural sands
250870	Clays (excluding expanded clays of heading no. 6806); chamotte or dinas earths
250620	Quartzite; whether or not roughly trimmed or merely cut, by sawing or otherwise, into blo...
280000	**Inorganic chemicals**
283911	Silicates; sodium metasilicates
281520	Potassium hydroxide (caustic potash)
281830	Aluminium hydroxide
820000	**Tools, implements, cutlery, spoons and forks, of base metal; parts thereof, of base metal**
821195	Knives; with handles of base metal
820770	Tools, interchangeable; (for machine or hand tools, whether or not power-operated), for m...
821490	Cutlery; hair clippers and mincing knives
870000	**Vehicles; other than railway or tramway rolling stock, and parts and accessories thereof**
870390	Vehicles; for transport of persons (other than those of heading no. 8702) n.e.c. in headi...
870590	Vehicles; break-down lorries, road-sweepers, spraying lorries, mobile workshops, mobile r...
870990	Vehicles; parts of the vehicles of heading no. 8709
730000	**Iron or steel articles**
730439	Iron or non-alloy steel (excluding cast iron); seamless, (excluding cold-drawn or cold-ro...
732211	Radiators and parts thereof; for central heating, (not electrically heated), of cast iron
730431	Iron or non-alloy steel (excluding cast iron); seamless, cold-drawn or cold-rolled, tubes...

Table 2: Top COD-intensive Products

HS Code	Description
380000	**Chemical products n.e.c.**
380400	Lyes, residual; from the manufacture of wood pulp, whether or not concentrated, desugared...
380892	Fungicides; other than containing goods specified in Subheading Note 1 to this Chapter; p...
381190	Oxidation and gum inhibitors, viscosity improvers, anti-corrosive preparations, other pre...
280000	**Inorganic chemicals**
282732	Chlorides; of aluminium
282741	Chloride oxides and chloride hydroxides; of copper
282510	Hydrazine and hydroxylamine and their inorganic salts
480000	**Paper and paperboard**
480421	Kraft paper and paperboard; sack kraft paper, uncoated, unbleached, in rolls or sheets, o...
480530	Paper and paperboard; sulphite wrapping paper, uncoated, in rolls or sheets
480620	Paper; greaseproof papers, in rolls or sheets
540000	**Man-made filaments and textile materials**
540234	Yarn, synthetic; filament, monofilament (less than 67 decitex), textured, of polypropylen...
540331	Yarn, artificial; filament, monofilament (less than 67 decitex), of viscose rayon (not hi...
540310	Yarn, artificial; filament, monofilament (less than 67 decitex), of high tenacity viscose...
410000	**Raw hides, skins and leather**
410632	Tanned or crust hides and skins; of swine, without hair on, whether or not split, but not...
410622	Tanned or crust hides and skins; of goats or kids, without hair on, whether or not split,...
411320	Leather; further prepared after tanning or crusting, including parchment-dressed leather,...
290000	**Organic chemicals**
293391	Heterocyclic compounds; n.e.c. in headings no. 2933.1, 2933.2, 2933.3, 2933.4, 2933.5, 29...
292214	Amino-alcohols, other than those containing more than one kind of oxygen function; their ...
292243	Amino-acids, other than those containing more than one kind of oxygen function, and their...

2.4 Robustness Check and Additional Results

2.4.1 Initial Guess of ζ_h

In our baseline estimation, we assign a uniform initial guess of $\zeta_h = 1$. To assess the robustness of this choice, we randomize the initial values of ζ_h by drawing from a uniform distribution over $[0.1, 5]$. This procedure generates 500 independent sets of estimates, each starting from a different random initialization. Despite this variation, the median pairwise correlation across all resulting estimates is 1.00 for every pollutant, indicating that our PLEI estimates are highly robust to the choice of initial values.[20]

2.4.2 Time Consistency of ζ_h

We operate under the assumption that PLEI captures the inherent, time-invariant production characteristics of individual products. In Appendix E, we assess the validity of this assumption and summarize the findings here.

We begin with the converged ζ_h and apply a single iteration of the algorithm described in Section 2.2 using data from year t to obtain $\zeta_{ht}^{[1]}$. If the full iteration were continued, it would yield the year-specific converged value $\zeta_{ht}^{[\infty]}$. If this value differs substantially from ζ_h, we would also expect $\zeta_{ht}^{[1]}$ to diverge much from ζ_h. Hence, the proximity between ζ_h and $\zeta_{ht}^{[1]}$ serves as a diagnostic for the temporal stability of PLEI.[21]

As shown in Appendix Table E.1, we find that $\zeta_{ht}^{[1]}$ aligns closely with ζ_h across years. In regressions of $\ln(\zeta_{ht})$ on $\ln(\zeta_h)$, the estimated slope coefficients consistently approximate 1.00, with standard errors below 0.01. These findings support the use of time-invariant PLEI as a parsimonious representation of emission characteristics over time, while allowing λ_{it} to capture firm-level improvements in abatement or efficiency.

[20] Detailed results are available upon request.

[21] The year-specific PLEI $\zeta_{ht}^{[\infty]}$ is estimated from a much smaller sample and is not comparable across years. These two limitations preclude a direct comparison between $\zeta_{ht}^{[\infty]}$ and ζ_h.

2.4.3 Distribution of λ_{it}

Our algorithm to estimate PLEI does not require any prior knowledge of λ_{it}, the firm-specific emission inefficiency parameter, nor does it generate λ_{it} as an intermediate step. However, once PLEI are determined, we can infer the λ_{it} value for each firm-year observation based on the following equation:

$$z_{it} = \lambda_{it} y_{it} \sum_h s_{hit} \zeta_h,$$

where s_{hit} represents the output value share of product h for firm i in year t. The expression $y_{it} \sum_h s_{hit} \zeta_h$ represents the predicted emissions attributable to the firm's output, product mix, and the PLEI for a representative firm whose λ_{it} equals 1. Consequently, λ_{it} can be interpreted as a ratio, comparing the firm's actual emissions to the hypothetical emissions level of a representative firm with an identical product mix.

Although a detailed exploration of λ_{it}'s nature falls outside the scope of this paper, we identify and describe key trends associated with λ_{it} in Figure 2.[22] Specifically, we observe that the firm-year emission inefficiency parameter λ_{it}: (1) shows a consistent downward trend over time, (2) tends to be lower among firms with higher productivity, and (3) is typically higher for state-owned enterprises (SOEs). These observations might indicate an overall enhancement in productivity and emission reduction efforts among Chinese firms over time. Additionally, the disparity between SOEs and non-SOEs could be attributed to productivity differences and stricter regulatory compliance required for non-SOEs. We conclude that the patterns in Figure 2 closely align with existing literature, reinforcing the credibility of our PLEI estimates from which firm-level λ_{it} are derived.

[22] As mentioned, λ_{it} serves as a comprehensive term for various determinants of firm-level emission intensities, including productivity (Shapiro and Walker, 2018), emissions abatement (Forslid et al., 2018; Kwon et al., 2023), market power (Rodrigue et al., 2022b), and regulatory stringency (He et al., 2020).

Figure 2: Distribution of λ_{it} by Productivity and Ownership (CO_2)

(a) By Productivity

(b) By Ownership

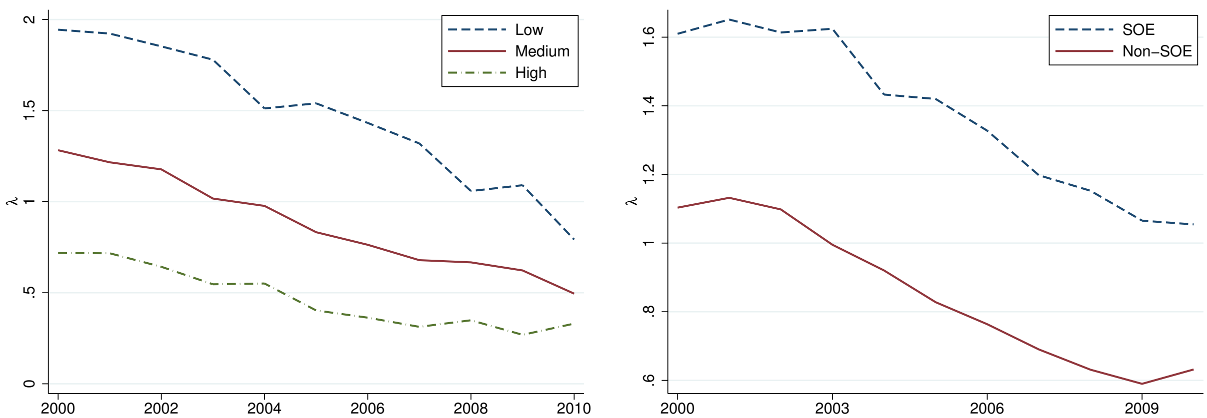

Notes: These figures show the distribution of Chinese firms' emission inefficiency parameter λ_{it} by the level of productivity (left) and ownership (right).

3 Stylized Facts about the PLEI

This section highlights key stylized facts regarding the PLEI. All analyses in this section are based on total emission intensities.

Stylized Fact 1: PLEI exhibit a striking degree of heterogeneity.

The most salient feature of PLEI is their pronounced variation across products. To illustrate, we normalize the maximum PLEI value for each pollutant to 100 and plot the distribution of the normalized PLEI in Figure 3. Even among the top 0.5% of emission-intensive products (roughly 20 products), emission intensities vary substantially. Products below the top 1% threshold exhibit negligible emission levels relative to the most emission-intensive products. This extreme dispersion is corroborated by Gini coefficients exceeding 0.95 for all pollutants.

A direct implication concerns the empirical design of studies in the trade-and-environment literature. A recurring challenge is that sector-level variation may be insufficient to identify causal effects, as industries differ not only in emission intensities but also along many

Figure 3: Skewness of Emission Intensities across 6-digit HS Code Products

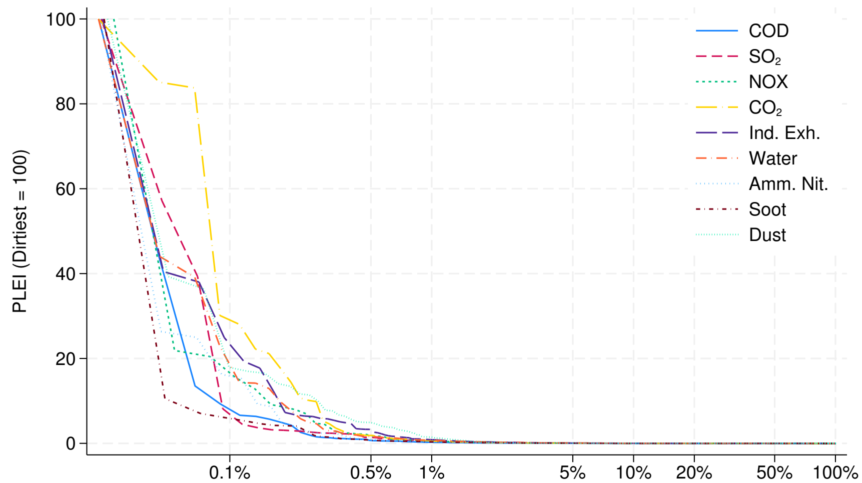

Notes: This figure illustrates the PLEI for nine pollutants in descending order. The highest PLEI for each pollutant is normalized to 100. The horizontal axis is log-scaled after multiplying 100.

unobserved dimensions (Grossman and Krueger, 1991; Ederington et al., 2005; Shapiro, 2021). Our findings suggest that (1) sectoral emission intensity may contain substantial aggregation bias, hindering identification; and (2) leveraging PLEI measures alongside industry fixed effects can help control for unobserved sector-level confounders, enabling more efficient empirical strategies.[23]

Stylized Fact 2: The top 10% of emission-intensive products account for nearly 75% of total emissions but comprise only 4% of China's export value.

Table 3 provides a detailed breakdown of emissions and export volumes for different product groups. Panel A, where products are ranked and grouped based on their emission intensities, reveals a striking fact that the top 1% of the most emission-intensive products contribute, on average, to nearly 34% of total emissions across various pollutants. The cumulative impact of the top 10% of emission-intensive products, which

[23]For example, Copeland et al. (2022) highlight the limited empirical support for the pollution haven hypothesis, partly due to the lack of observed composition effects at the sectoral level. The substantial product-level heterogeneity uncovered in our study suggests that aggregation bias may mask these effects, and that exploiting product-level variation in composition may offer a promising direction for future research.

encompasses approximately 440 items, is responsible for nearly 75% of total emissions (summing the first three rows). Conversely, as detailed in the lower section of Panel A, these top 1% and 10% of emission-intensive products account for merely 0.13% and 3.82% of China's total export volume, respectively. This marked imbalance underscores the significant potential of our PLEI measure to guide efficient tax policy. Specifically, our stylized facts 1 and 2 suggest that environment tax targeted at a small number of emission-intensive products can effectively reduce emissions while causing minimum economic distortion.

Panel B of Table 3 provides a slightly different perspective by categorizing products according to their total emissions. As anticipated, the proportion of emissions attributed to top products and their export volume both increase compared with Panel A. Still, a similar critical observation from Panel B is the concentration of emissions within a narrow product range: the top 10% of products are responsible for over 90% of the total emissions.

Table 3: Percentage of Total Emissions Accounted For by Top Emission-intensive 6-digit HS Code Products

	AVG	*CO_2*	*COD*	*SO_2*	*NOX*	*Exh.*	*Water*	*Amm.*	*Soot*	*Dust*
Panel A. Product Ranking Based on Emission Intensities										
pct. of emissions										
top 1 pct. HS	33.82	69.89	27.17	16.93	18.55	26.98	20.54	21.22	20.78	69.71
next 4 pct. HS	26.13	9.18	24.10	29.53	22.39	36.37	27.00	12.49	39.92	20.51
next 5 pct. HS	11.44	3.84	15.78	13.09	18.76	9.50	17.27	5.67	11.25	2.00
next 40 pct. HS	17.36	13.01	22.95	22.59	26.56	20.77	19.72	30.96	10.39	2.89
bottom 50 pct. HS	11.26	4.08	10.00	17.86	13.74	6.38	15.47	29.65	17.65	4.90
pct. of exports										
top 1 pct. HS	0.13	0.12	0.11	0.07	0.15	0.12	0.13	0.21	0.07	0.23
next 4 pct. HS	1.05	0.98	0.66	0.81	0.99	1.20	1.06	0.69	1.07	1.60
next 5 pct. HS	2.64	1.90	1.47	1.58	1.61	2.52	1.60	1.33	2.14	8.28
next 40 pct. HS	35.88	60.02	49.01	26.41	35.12	31.06	38.76	41.53	19.43	27.19
bottom 50 pct. HS	60.32	36.99	48.75	71.13	62.13	65.11	58.46	56.25	77.29	62.70
Panel B. Product Ranking Based on Total Emissions										
pct. of emissions										
top 1 pct. HS	58.49	78.52	50.40	44.33	52.82	57.25	50.13	47.44	53.00	81.44
next 4 pct. HS	24.55	12.49	28.13	30.41	27.78	27.87	29.40	25.61	26.77	13.58
next 5 pct. HS	7.52	3.81	9.67	10.83	8.27	7.64	9.19	10.33	8.63	2.11
next 40 pct. HS	8.82	4.83	11.20	13.45	10.28	6.86	10.50	15.26	10.77	2.64
bottom 50 pct. HS	0.63	0.35	0.60	0.98	0.86	0.38	0.78	1.35	0.83	0.24
pct. of exports										
top 1 pct. HS	11.18	15.36	15.54	15.60	16.01	4.67	15.59	21.05	6.21	0.49
next 4 pct. HS	19.78	20.85	15.58	15.30	14.62	16.76	18.21	19.85	22.79	34.10
next 5 pct. HS	15.81	15.87	12.50	16.05	14.92	17.25	15.98	12.81	17.12	16.80
next 40 pct. HS	41.87	38.70	45.76	42.06	39.97	48.81	40.44	36.67	41.64	37.56
bottom 50 pct. HS	11.35	9.21	10.60	10.98	14.47	12.51	9.78	9.62	12.23	11.05
HS products	.	4482	4460	4336	3757	4262	4473	4383	4195	4036

Notes: The table presents a breakdown of emissions associated with the most emission-intensive products, classified at the 6-digit HS code level. Panel A reports the share of total emissions and exports accounted for by the top emission-intensive HS codes, while Panel B presents the same for HS codes with the highest absolute emission levels. The "AVG" column shows the average across nine pollutants for each row.

Stylized Fact 3: Broad product categories significantly underestimate the heterogeneity in emission intensities.

Emission intensities are often calculated at the sector level or broad product classifications, such as HS 2-digit categories. When PLEI exhibit substantial within-group variation, such aggregation can significantly understate heterogeneity across products.

Figure 4 illustrates this point by plotting the cumulative distribution of CO_2 emissions against export volume, with products ordered by ascending emission intensity.[24] The contrast is striking: at the HS 6-digit level, the curve rises sharply, with approximately 80 percent of emissions originating from less than 3% of trade volume (see Table 3). In contrast, HS 2-digit aggregation yields a much flatter curve, attributing the same share of emissions to nearly 30% of trade volume. These patterns underscore the importance of using disaggregated data to accurately characterize the distribution of emissions across traded products.

A key implication for environmental policy is the benefit of a detailed Pigouvian tax schedule that reflects product-level variation in PLEI.[25] Specifically, if CBAM is implemented by assigning tax rates to product groups, Figure 4 suggests that doing so at the HS 6-digit level would yield substantially greater efficiency than aggregation at the HS 2-digit level.

However, this analysis does not account for the full range of economic consequences associated with product- versus sector-based CBAM. In particular, it abstracts from input-output linkages and general equilibrium effects operating through income channels and third-country markets. We address these limitations in Section 4, where we compare the effectiveness and economic efficiency of product- and sector-level CBAM policies within

[24] Results for other pollutants are reported in Appendix F.

[25] In principle, a first-best policy would tax each product—or even each variety—according to its exact emissions content, accounting for firm-level efficiency differences. In practice, however, such precision is rarely feasible, as it relies on truthful reporting and verifiable measurement. These challenges are further magnified under CBAM, where production and taxation occur in different jurisdictions. For this reason, we posit that CBAM implementation is likely to resemble the existing tariff system, in which an ad valorem rate is applied to each product category.

a general equilibrium trade model.

Figure 4: Cumulative Total Emissions and Trade Volume (CO_2)

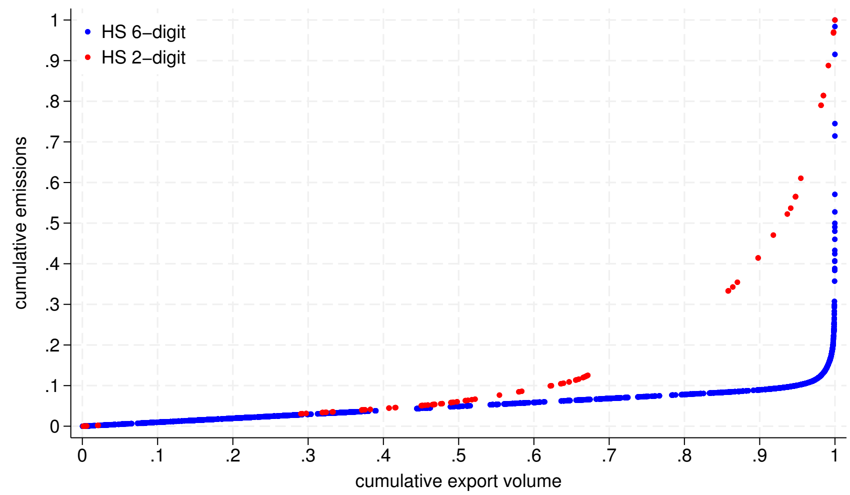

Notes: This figure illustrates the cumulative distributions of total emissions and export volumes. Products are ranked in the increasing order of their total emission intensities.

Stylized Fact 4: Chinese exports are less carbon-intensive than its imports and global trade flows. From 2000 to 2013, carbon-intensive exports grew more slowly than non-intensive ones.

To illustrate Stylized Fact 4, we introduce a product group based on their CO_2 intensities. Specifically, we define a product as *carbon-intensive* if its CO_2 emission intensity falls within the top decile of the distribution.

Using our PLEI estimates, we examine the evolution of China's trade patterns with respect to carbon-intensive goods. The left panel of Figure 5 reports the share of carbon-intensive products in China's exports, imports, and global trade flows.[26] Under the Pollution Haven Hypothesis (PHH; Copeland and Taylor, 1994), one might expect China to increasingly specialize in carbon-intensive exports following its accession to the WTO in

[26]Our classification of carbon-intensive products is based on China's production processes. Ideally, with comparable data across countries, carbon intensity would be defined separately for imports and exports based on the origin. We assume that products emission-intensive in Chinese production are also likely to be emission-intensive abroad. In Appendix D, we show that emission intensities are highly correlated across countries at the sectoral level, with correlation coefficients generally exceeding 0.6.

2001, given its relatively lax environmental regulations. However, the data reveal no such trend: between 2000 and 2013, the share of carbon-intensive products in China's exports (red dashed line) remains relatively stable, providing no empirical support for the PHH.

Figure 5: Emissions in Chinese Trade, Imports vs. Exports (CO_2)

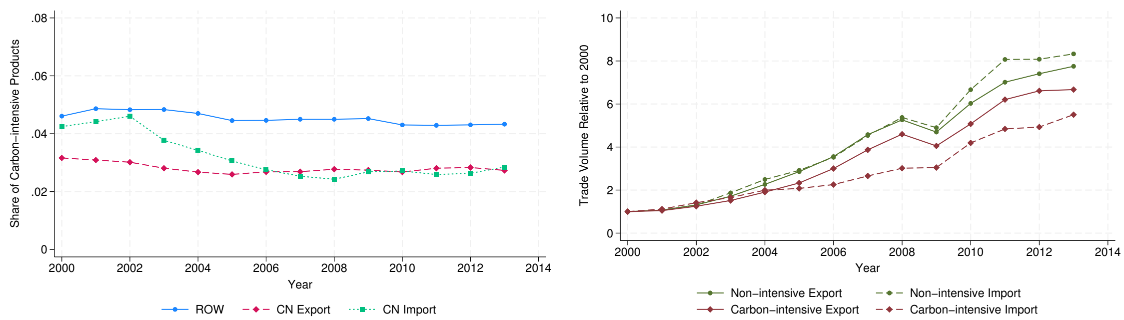

Notes: The left figure presents the trade share of carbon-intensive products, defined as those in the top 10% of CO_2 emission intensities, within China's exports, imports, and global trade flows. The right figure plots the growth trajectory of both non-intensive and carbon-intensive product imports and exports since 2000.

Paradoxically, the share of carbon-intensive products in China's imports (green dotted line), expected to be lower under the PHH, was higher than that in exports prior to 2006 and roughly comparable thereafter. This pattern is reminiscent of the Leontief paradox (Leontief, 1953), in which the U.S. was found to import capital-intensive goods. Perhaps even more striking, the share of carbon-intensive products in the rest of the world's trade (blue solid line) consistently exceeds that in both China's exports and imports.

The right panel of Figure 5 illustrates the evolution of China's imports and exports for carbon-intensive versus non-intensive products since 2000. Most notably, non-intensive exports grew faster than carbon-intensive exports, contrary to the predictions of the PHH. On the import side, non-intensive products also grew more rapidly than carbon-intensive ones, a pattern more consistent with the PHH. Taken together, the mixed patterns in Figure 5 offer limited support for the notion that China became disproportionately specialized in carbon-intensive exports following its accession to the WTO.[27]

[27] A full assessment of the PHH is beyond the scope of this paper, but related studies on China report

4 An Application to the CBAM

This section demonstrates how PLEI can inform the design of a more economically efficient CBAM policy. In the main text, we briefly outline the model, data, and methodology used in the counterfactual analysis, deferring full details to Appendix G.

4.1 An Overview of the Quantitative Framework

To assess the implications of PLEI for CBAM design, we employ a multi-country general equilibrium trade model. Building on Duan et al. (2021), the model incorporates emissions as a production factor, consistent with the dual-role interpretation in Copeland and Taylor (1994), and embeds this feature in a Ricardian structure following Caliendo and Parro (2015).[28]

In addition to the data described in Section 2.1, we use the World Input-Output Database (WIOD) to obtain information on value added, input-output linkages, and final demand across countries and sectors (Timmer et al., 2015). All data used for the CBAM simulation are benchmarked to the year 2007. Emission elasticities and implicit domestic carbon prices are inferred from WIOD environmental accounts.[29] Trade elasticities at the HS 6-digit level are taken from Fontagné et al. (2022), with sectoral elasticities computed as medians across constituent products. Bilateral tariffs are obtained from MAcMap-HS6 (Guimbard et al., 2012).

For computational feasibility, we aggregate the world into three regions — China, the EU, and the rest of the world.[30] Sector-level simulations include 21 tradable and 10 non-tradable sectors. At the product level, simulations include 1,134 dirty products, 21

similar mixed findings. For example, Duan et al. (2021) conclude that environmental policy has played only a limited role in shaping China's trade specialization.

[28] Copeland and Taylor (1994) conceptualize emissions both as a by-product and as a productive input.

[29] We compute emission elasticities following Duan et al. (2021), using the OECD Environmental Policy Stringency Index (Botta and Koźluk, 2014), environmental tax revenue accounts, and the Environmental Regulatory Regimes Index (Esty and Porter, 2001).

[30] Figure G.1 confirms that sectoral CBAM results are robust to regional aggregation.

clean products, and 10 non-tradable sectors.[31] Counterfactual analysis employs "exact hat algebra" (Dekle et al., 2008), thereby avoiding the need to calibrate unobserved structural parameters such as absolute trade costs and productivity.

4.2 CBAM Counterfactual Analysis

Using the calibrated model, we conduct counterfactual simulations to quantify the efficiency gains from incorporating PLEI into CBAM policy design.[32] We examine two policy scenarios. In the benchmark counterfactual, the EU imposes a carbon border tax on imports from China in the seven most carbon-intensive tradable sectors.[33] The EU adopts a uniform carbon price which—when multiplied by sectoral emission intensities—yields sector-specific ad valorem CBAM tariffs. We refer to this policy as *sector-level CBAM*.

In the alternative counterfactual, the EU imposes CBAM tariffs on all Chinese HS 6-digit products with carbon emissions. As in the benchmark case, the EU sets a single carbon price, which yields product-specific ad valorem CBAM tariffs when multiplied by the PLEI. We refer to this policy as *product-level CBAM*.

Figures 6 and 7 illustrate the outcomes under sector- and product-level CBAM, respectively. Under sector-level CBAM (Figure 6), higher carbon prices reduce both the volume of Chinese exports to the EU and the emissions embedded in those exports. At a carbon price of $80 per ton, export volume declines by 4.93 percent, while associated emissions fall by 40.9 percent. The relatively larger drop in emissions reflects the proportional na-

[31] In the CBAM simulation, we classify products as "dirty" if they exhibit positive PLEI, and as "clean" if their PLEI equal zero. Within each WIOD sector, clean products are aggregated to a single representative product for computational efficiency.

[32] Throughout, we vary the EU's carbon tax on imports from China only, leaving tariffs among other trading partners unchanged. Extending the analysis to other EU trade partners would require stronger assumptions on the cross-country comparability of PLEI. We also abstract from EU export rebates as a component of border adjustments.

[33] The sectors include: Mining and quarrying; Manufacture of food, beverages, and tobacco; Paper and paper products; Chemicals; Non-metallic mineral products; Basic metals. These align with the sectors identified in the European Parliament's CBAM proposal: "The sectors covered by the CBAM are cement, electricity, fertilisers, iron and steel, and aluminium hydrogen, and some precursors and downstream products made from cement, iron and steel, and aluminium" (European Parliament, 2023).

Figure 6: Effect of Sector-Level CBAM on Trade and Emissions

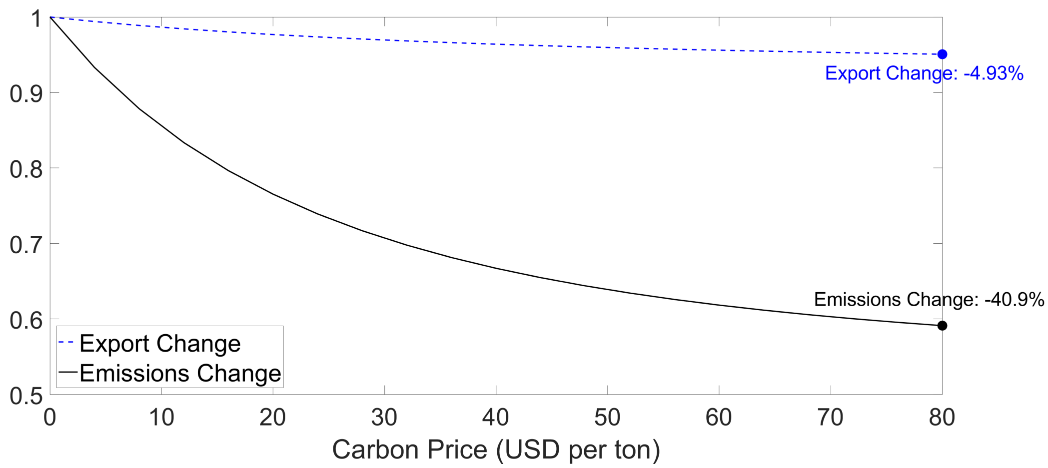

Notes: This figure illustrates changes in China-to-EU exports and associated emissions under the sector-level CBAM regime, across a range of carbon prices.

ture of the tax: carbon-intensive sectors face higher ad valorem tariffs at a given carbon price.

In contrast, product-level CBAM (Figure 7) achieves substantially greater emissions reductions at markedly lower trade costs. At the same carbon price of $80 per ton, embedded emissions fall by 88.7 percent, while trade volume declines by only 1.16 percent. The efficiency gain stems from the granularity of product-level targeting: CBAM tariffs rise steeply for the most carbon-intensive products and remain low for cleaner goods. By contrast, sector-level CBAM obscures this heterogeneity, under-taxing high-emission products and over-taxing low-emission ones within a given sector, thereby exacerbating economic distortions.

Figure 8 offers an alternative approach to compare the two CBAM regimes. The horizontal axis reports reductions in embedded emissions, while the vertical axis captures the corresponding declines in Chinese exports to the EU. As can be seen, sector-level CBAM entails substantially greater trade reductions for any given level of emissions abatement. Strikingly, product-level CBAM achieves the same emissions reduction attained by sector-level CBAM at $80 per ton with a carbon price of just $4 per ton! The underlying mech-

Figure 7: Effect of Product-Level CBAM on Trade and Emissions

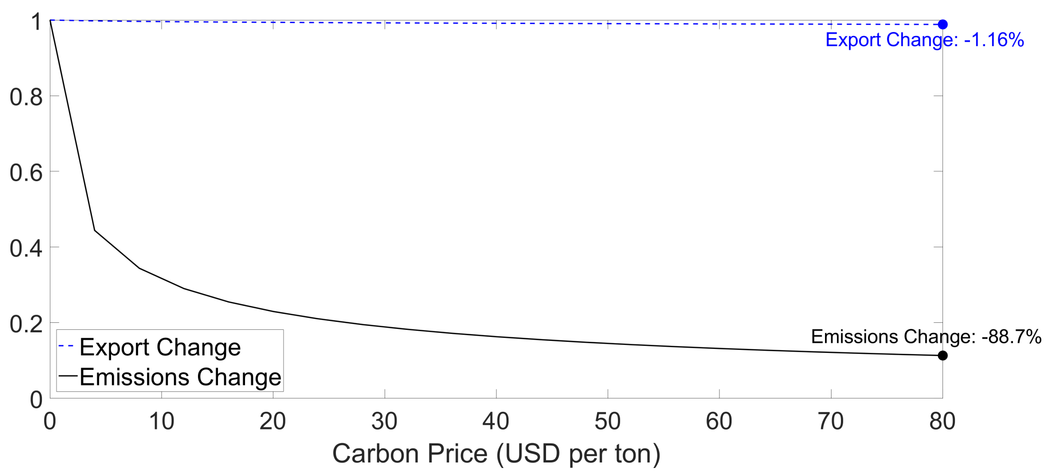

Notes: This figure illustrates changes in China-to-EU exports and associated emissions under the product-level CBAM regime, across a range of carbon prices.

anism is as previously discussed: product-level CBAM more precisely targets high-PLEI products, generating large ad valorem tariffs even at low carbon prices. The low carbon price, in turn, limits economic distortion by avoiding over-taxation of low-emission products in high-emission sectors.

Finally, Figure 9 compares real consumption in China and the EU under each policy regime.[34] Notably, at a carbon price of $80 per ton, China's real consumption loss under product-level CBAM is 73.7 percent lower than under sector-level CBAM, comparing the right endpoints of the dashed and solid black lines. The EU, by contrast, enjoys higher real consumption under sector-level CBAM. This asymmetry reflects the EU's ability to exploit terms-of-trade gains by raising tariffs more aggressively under sector-level CBAM (Johnson, 1953; Ossa, 2014; Bagwell et al., 2021). However, this gain in consumption comes at the cost of substantially lower emissions reductions: at $80 per ton, sector-level CBAM yields a 40.9 percent reduction, compared to 88.7 percent under product-level

[34]Following standard practice in the trade literature, we use real consumption as a proxy for welfare (Costinot and Rodríguez-Clare, 2014). We note, however, that in the trade-and-environment literature, welfare may also include disutility from emissions (Copeland and Taylor, 1994, 2003, 2004). To account for this, we compare changes in real consumption between two policy regimes, conditional on achieving the same reduction in emissions.

Figure 8: Sector-Level vs. Product-Level CBAM: Trade and Emissions

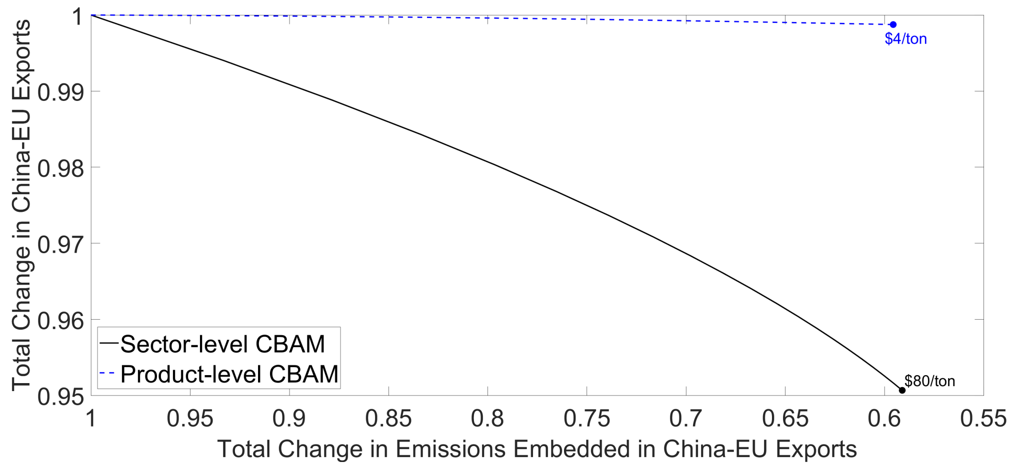

Notes: This figure compares sector- and product-level CBAM policies by depicting the decline in China-to-EU exports relative to the corresponding reduction in embedded emissions. Each point along the lines represents the associated changes in exports and embedded emissions across varying carbon prices.

Figure 9: Sector-Level vs. Product-Level CBAM: Real Consumption

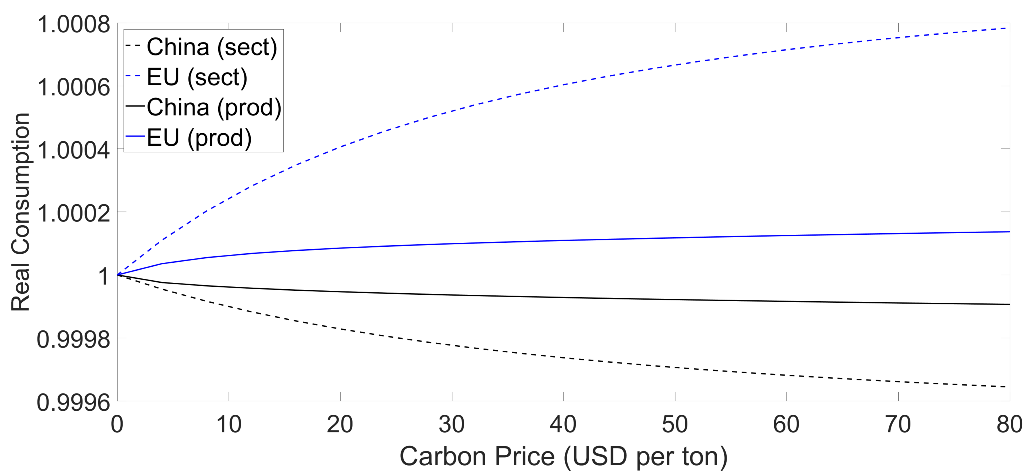

Notes: This figure compares the effects of sector- and product-level CBAM policies on real consumption for China and the EU.

CBAM.

5 Conclusion

This paper develops a new methodology for estimating product-level emission intensities (PLEI) using firm-product-level output and firm-level emissions data. The proposed iterative approach consistently accounts for emissions by multi-product firms and is broadly applicable due to its modest data requirements.

Applying the method to Chinese firm-level data from 2000 to 2013, we find that the top decile of emission-intensive product categories accounts for approximately 75 percent of total emissions embodied in exports, while comprising less than 4 percent of export volume. We further show that incorporating PLEI into the design of CBAM enables substantially greater emission reductions with lower trade disruption relative to conventional sector-based approaches. We believe that our methodology and findings offer valuable inputs for empirical research and the design of environmental trade policies.

References

AICHELE, R. AND G. FELBERMAYR (2015): "Kyoto and Carbon Leakage: An Empirical Analysis of the Carbon Content of Bilateral Trade," *The Review of Economics and Statistics*, 97, 104–115.

BAGWELL, K., R. W. STAIGER, AND A. YURUKOGLU (2021): "Quantitative Analysis of Multiparty Tariff Negotiations," *Econometrica*, 89, 1595–1631.

BALISTRERI, E. J., D. T. KAFFINE, AND H. YONEZAWA (2019): "Optimal Environmental Border Adjustments Under the General Agreement on Tariffs and Trade," *Environmental and Resource Economics*, 74, 1037–1075.

BARROWS, G. AND H. OLLIVIER (2018): "Cleaner Firms or Cleaner Products? How Product Mix Shapes Emission Intensity from Manufacturing," *Journal of Environmental Economics and Management*, 88, 134–158.

BELLORA, C. AND L. FONTAGNÉ (2023): "EU in Search of a Carbon Border Adjustment Mechanism," *Energy Economics*, 123, 106673.

BERNARD, A. B., S. J. REDDING, AND P. K. SCHOTT (2010): "Multiple-Product Firms and Product Switching," *American Economic Review*, 100, 70–97.

——— (2011): "Multiproduct Firms and Trade Liberalization," *The Quarterly Journal of Economics*, 126, 1271–1318.

BÖHRINGER, C., J. C. CARBONE, AND T. F. RUTHERFORD (2016): "The Strategic Value of Carbon Tariffs," *American Economic Journal: Economic Policy*, 8, 28–51.

BÖHRINGER, C., A. LANGE, AND T. F. RUTHERFORD (2014): "Optimal Emission Pricing in the Presence of International Spillovers: Decomposing Leakage and Terms-of-Trade Motives," *Journal of Public Economics*, 110, 101–111.

Botta, E. and T. Koźluk (2014): "Measuring Environmental Policy Stringency in OECD Countries," *OECD*.

Caliendo, L. and F. Parro (2015): "Estimates of the Trade and Welfare Effects of NAFTA," *The Review of Economic Studies*, 82, 1–44.

Cherniwchan, J. (2017): "Trade Liberalization and the Environment: Evidence from NAFTA and U.S. Manufacturing," *Journal of International Economics*, 105, 130–149.

Cherniwchan, J., B. R. Copeland, and M. S. Taylor (2017): "Trade and the Environment: New Methods, Measurements, and Results," *Annual Review of Economics*, 9, 59–85.

Choi, J., J. Hyun, G. Kim, and Z. Park (2025): "The Cleanup of US Manufacturing through Pollution Offshoring," *Journal of International Economics*, 154, 104046.

Copeland, B. R., J. S. Shapiro, and M. Scott Taylor (2022): "Globalization and the Environment," in *Handbook of International Economics*, ed. by G. Gopinath, E. Helpman, and K. Rogoff, Elsevier, vol. 5 of *Handbook of International Economics: International Trade, Volume 5*, 61–146.

Copeland, B. R. and M. S. Taylor (1994): "North-South Trade and the Environment," *The Quarterly Journal of Economics*, 109, 755–787.

——— (2003): "Trade and the Environment: Theory and Evidence," in *Trade and the Environment*, Princeton University Press.

——— (2004): "Trade, Growth, and the Environment," *Journal of Economic Literature*, 42, 7–71.

Costinot, A. and A. Rodríguez-Clare (2014): "Chapter 4 - Trade Theory with Numbers: Quantifying the Consequences of Globalization," in *Handbook of International Eco-*

nomics, ed. by G. Gopinath, E. Helpman, and K. Rogoff, Elsevier, vol. 4 of *Handbook of International Economics*, 197–261.

DEKLE, R., J. EATON, AND S. KORTUM (2008): "Global Rebalancing with Gravity: Measuring the Burden of Adjustment," *IMF Staff Papers*, 55, 511–540.

DIETZENBACHER, E., J. PEI, AND C. YANG (2012): "Trade, Production Fragmentation, and China's Carbon Dioxide Emissions," *Journal of Environmental Economics and Management*, 64, 88–101.

DUAN, Y., T. JI, Y. LU, AND S. WANG (2021): "Environmental Regulations and International Trade: A Quantitative Economic Analysis of World Pollution Emissions," *Journal of Public Economics*, 203, 104521.

EATON, J. AND S. KORTUM (2002): "Technology, Geography, and Trade," *Econometrica*, 70, 1741–1779.

EDERINGTON, J., A. LEVINSON, AND J. MINIER (2005): "Footloose and Pollution-Free," *The Review of Economics and Statistics*, 87, 92–99.

ESTY, D. C. AND M. E. PORTER (2001): "Ranking National Environmental Regulation and Performance: A Leading Indicator of Future Competitiveness?" *The Global Competitiveness Report*, 78–100.

EUROPEAN PARLIAMENT, . (2023): "Carbon Border Adjustment Mechanism," *European Parliamentary Research Service*.

FAN, H., J. GRAFF ZIVIN, Z. KOU, X. LIU, AND H. WANG (2025): "Going Green in China: Firms' Responses to Stricter Environmental Regulations," *Canadian Journal of Economics/Revue canadienne d'économique*, 58, 385–410.

FARROKHI, F. AND A. LASHKARIPOUR (2025): "Can Trade Policy Mitigate Climate Change?" *Working Paper*.

FONTAGNÉ, L., H. GUIMBARD, AND G. OREFICE (2022): "Tariff-Based Product-Level Trade Elasticities," *Journal of International Economics*, 137, 103593.

FONTAGNÉ, L. AND K. SCHUBERT (2023): "The Economics of Border Carbon Adjustment: Rationale and Impacts of Compensating for Carbon at the Border," *Annual Review of Economics*, 15, 389–424.

FORSLID, R., T. OKUBO, AND K. H. ULLTVEIT-MOE (2018): "Why Are Firms That Export Cleaner? International Trade, Abatement and Environmental Emissions," *Journal of Environmental Economics and Management*, 91, 166–183.

FRANKEL, J. (2009): "Environmental Effects of International Trade," Scholarly Articles, Harvard Kennedy School of Government.

GAULIER, G. AND S. ZIGNAGO (2010): "BACI: International Trade Database at the Product-Level. The 1994-2007 Version," *Working Papers*.

GROSSMAN, G. M. AND A. B. KRUEGER (1991): "Environmental Impacts of a North American Free Trade Agreement," *NBER Working Paper*.

GUIMBARD, H., S. JEAN, M. MIMOUNI, AND X. PICHOT (2012): "MAcMap-HS6 2007, An Exhaustive and Consistent Measure of Applied Protection in 2007," *International Economics*, 130, 99–121.

HE, G., S. WANG, AND B. ZHANG (2020): "Watering Down Environmental Regulation in China," *The Quarterly Journal of Economics*, 135, 2135–2185.

JOHNSON, H. G. (1953): "Optimum Tariffs and Retaliation," *The Review of Economic Studies*, 21, 142–153.

KEEN, M. AND C. KOTSOGIANNIS (2014): "Coordinating Climate and Trade Policies: Pareto Efficiency and the Role of Border Tax Adjustments," *Journal of International Economics*, 94, 119–128.

KLOTZ, R. AND R. R. SHARMA (2023): "Trade Barriers and CO2," *Journal of International Economics*, 141, 103726.

KORTUM, S. AND D. A. WEISBACH (2023): "Optimal Unilateral Carbon Policy," *Cowles Foundation Discussion Paper No. 2311*.

KWON, O., H. ZHAO, AND M. Q. ZHAO (2023): "Global Firms and Emissions: Investigating the Dual Channels of Emissions Abatement," *Journal of Environmental Economics and Management*, 118, 102772.

LARCH, M. AND J. WANNER (2017): "Carbon Tariffs: An Analysis of the Trade, Welfare, and Emission Effects," *Journal of International Economics*, 109, 195–213.

LEONTIEF, W. (1953): "Domestic Production and Foreign Trade; The American Capital Position Re-Examined," *Proceedings of the American Philosophical Society*, 97, 332–349.

——— (1970): "Environmental Repercussions and the Economic Structure: An Input-Output Approach," *The Review of Economics and Statistics*, 52, 262–271.

LEVINSON, A. (2009): "Technology, International Trade, and Pollution from US Manufacturing," *American Economic Review*, 99, 2177–2192.

——— (2023): "Are Developed Countries Outsourcing Pollution?" *Journal of Economic Perspectives*, 37, 87–110.

LIU, M., R. SHADBEGIAN, AND B. ZHANG (2017): "Does Environmental Regulation Affect Labor Demand in China? Evidence from the Textile Printing and Dyeing Industry," *Journal of Environmental Economics and Management*, 86, 277–294.

LYUBICH, E., J. SHAPIRO, AND R. WALKER (2018): "Regulating Mismeasured Pollution: Implications of Firm Heterogeneity for Environmental Policy," *AEA Papers and Proceedings*, 108, 136–142.

MELITZ, M. J. (2003): "The Impact of Trade on Intra-Industry Reallocations and Aggregate Industry Productivity," *Econometrica*, 71, 1695–1725.

NORDHAUS, W. (2015): "Climate Clubs: Overcoming Free-Riding in International Climate Policy," *American Economic Review*, 105, 1339–1370.

OSSA, R. (2014): "Trade Wars and Trade Talks with Data," *American Economic Review*, 104, 4104–4146.

ROBERTS, M. J., D. YI XU, X. FAN, AND S. ZHANG (2018): "The Role of Firm Factors in Demand, Cost, and Export Market Selection for Chinese Footwear Producers," *The Review of Economic Studies*, 85, 2429–2461.

RODRIGUE, J., D. SHENG, AND Y. TAN (2022a): "The Curious Case of the Missing Chinese Emissions," *Journal of the Association of Environmental and Resource Economists*, 9, 755–805.

——— (2022b): "Exporting, Abatement, and Firm-Level Emissions: Evidence from China's Accession to the WTO," *The Review of Economics and Statistics*, 1–45.

SHAPIRO, J. S. (2016): "Trade Costs, CO_2, and the Environment," *American Economic Journal: Economic Policy*, 8, 220–254.

——— (2021): "The Environmental Bias of Trade Policy," *The Quarterly Journal of Economics*, 136, 831–886.

SHAPIRO, J. S. AND R. WALKER (2018): "Why Is Pollution from US Manufacturing Declining? The Roles of Environmental Regulation, Productivity, and Trade," *American Economic Review*, 108, 3814–3854.

STAIGER, R. W. (2022): *A World Trading System for the Twenty-First Century*, MIT Press.

TANAKA, S., K. TESHIMA, AND E. VERHOOGEN (2022): "North-South Displacement Effects of Environmental Regulation: The Case of Battery Recycling," *American Economic Review: Insights*, 4, 271–288.

TIMMER, M. P., E. DIETZENBACHER, B. LOS, R. STEHRER, AND G. J. DE VRIES (2015): "An Illustrated User Guide to the World Input–Output Database: The Case of Global Automotive Production," *Review of International Economics*, 23, 575–605.

YU, M. (2015): "Processing Trade, Tariff Reductions and Firm Productivity: Evidence from Chinese Firms," *The Economic Journal*, 125, 943–988.

ZHANG, Q., X. JIANG, D. TONG, S. J. DAVIS, H. ZHAO, G. GENG, T. FENG, B. ZHENG, Z. LU, D. G. STREETS, R. NI, M. BRAUER, A. VAN DONKELAAR, R. V. MARTIN, H. HUO, Z. LIU, D. PAN, H. KAN, Y. YAN, J. LIN, K. HE, AND D. GUAN (2017): "Transboundary Health Impacts of Transported Global Air Pollution and International Trade," *Nature*, 543, 705–709.

Online Appendix:
Product Level Emission Intensities: Measurement and Application

by

Ohyun Kwon

Hao Zhao

Min Qiang Zhao

Table of Contents

A Theoretical Framework 2

B Monte Carlo Simulation for PLEI 11

B.1 Data Generating Process 11

B.2 Comparison Between Actual and Simulated Datasets 14

B.3 DGP-1: λ_i Varies Across Firms 17

B.4 DGP-2: λ_{hi} Varies Across Firms and Products 17

B.5 Regression Approach 19

C Verifying PLEI with External Datasets 22

D Cross-Country Comparison of Industrial-Level Emission Intensities 27

E Time Consistency of ζ_h 29

F Additional Tables and Figures 31

G Carbon Border Adjustment Mechanism 43

G.1 Model 43

G.2 Data 49

G.3 Regional and Product Aggregation 52

A Theoretical Framework

This section develops a theoretical framework for multiproduct firms, focusing on how firm-product-level emission intensities can be expressed as equation (1) in standard trade models. We also argue that firm-product-level productivity shocks can be treated as white noise that are not critical to PLEI esitmation as the number of firm size increases. For tractability, we consider a single destination market.

Consumer Preferences

We assume a representative consumer with preferences over a continuum of product categories indexed by $h \in [0, 1]$. The consumer's utility is a CES aggregate across product categories:

$$U = \left[\int_0^1 C_h^{\nu} \, dh \right]^{\frac{1}{\nu}}, \qquad 0 < \nu < 1,$$

where C_h denotes the consumption index for product category h.

Within each product category h, consumers choose among a continuum of horizontally differentiated varieties indexed by $\omega \in \Omega_h$. The consumption aggregator and the corresponding price index for category h follow the standard CES form:

$$C_h = \left[\int_{\omega \in \Omega_h} c_h(\omega)^{\rho} \, d\omega \right]^{\frac{1}{\rho}}, \qquad P_h = \left[\int_{\omega \in \Omega_h} p_h(\omega)^{1-\sigma} \, d\omega \right]^{\frac{1}{1-\sigma}}, \qquad 0 < \rho < 1,$$

where $\sigma > 1$ is the elasticity of substitution across varieties and is related to ρ by $\sigma = 1/(1 - \rho)$.

Firms and Product Varieties

Each firm i may enter a product market to produce a single variety within each product category h, incurring a sunk entry cost f_h for each market entered. Entry yields a distinct blueprint for a horizontally differentiated variety ω within the corresponding product space.

We treat total consumption C_h for each product category as given. Given the one-to-one mapping between firms i and varieties ω, the demand faced by firm i for its variety $\omega \in \Omega_h$ is:

$$c_h(\omega) = C_h P_h^{\sigma} \cdot p_h(\omega)^{-\sigma}. \tag{A.1}$$

Production Technology and Pricing

Upon incurring a firm-level fixed cost f_i, firm i draws its core productivity φ_i from a distribution $G_i(\varphi_i)$. It also draws a product-specific productivity φ_{ih} from $G_h(\varphi_{ih})$, satisfying $\mathbb{E}(\varphi_{ih}^{-1}) = 1$, which is equivalent to normalizing the unit labor requirement.[35]

Firms produce output using a Cobb–Douglas technology in clean input (labor) ℓ and emissions z:

$$q_{ih} = \varphi_i \cdot \Phi_h \varphi_{ih} \cdot \frac{\ell_{ih}^{1-\alpha_h} z_{ih}^{\alpha_h}}{(1-\alpha_h)^{1-\alpha_h} \alpha_h^{\alpha_h}}, \tag{A.2}$$

where ℓ_{ih} denotes the quantity of clean input and z_{ih} denotes emissions, following Copeland and Taylor (1994) and Φ_h is a product-specific scaling parameter that induces correlation in productivity across product categories. The parameter $\alpha_h \in (0,1)$ reflects the output elasticity with respect to emissions and captures the emission intensity of product category h.

Equation (A.2) generalizes standard formulations by allowing firm-product-specific productivity φ_{ih} to be correlated across firms via the common factor Φ_h, thereby relaxing

[35] To avoid confusion, we clarify that the subscript on the distribution G_h denotes that it pertains to all product-specific productivity, and does *not* imply that each product has a distinct distribution. The same interpretation applies to G_i.

the assumption of independence across product draws. The cost-minimizing combination of inputs required to produce one unit of output implies a unit cost given by:

$$\nu_h = w^{1-\alpha_h}\tau^{\alpha_h},$$

where w is the wage rate and τ denotes the emission tax or cost per unit of emissions.

Facing the residual demand in equation (A.1), firms set prices as a constant markup over marginal cost:

$$p_h(\varphi_i, \varphi_{ih}) = \frac{\nu_h}{\rho\varphi_i\Phi_h\varphi_{ih}}, \tag{A.3}$$

where the markup is determined by ρ, the elasticity parameter of the CES aggregator.

Substituting the pricing rule (A.3) into the demand function (A.1), the equilibrium quantity sold by firm i in product category h is:

$$q_h(\varphi_i, \varphi_{ih}) = C_h P_h^{\sigma} \cdot \left(\frac{\nu_h}{\rho\varphi_i\Phi_h\varphi_{ih}}\right)^{-\sigma}. \tag{A.4}$$

Firm Profits and Entry Decision

The operating profit of a firm from producing variety ω in product category h is given by the difference between revenue and input costs $\pi_h = p_h \cdot q_h - w \cdot \ell_h - \tau \cdot z_h$.

The zero-cutoff profit condition determines the minimum firm-product-level productivity $\varphi_{ih}^*(\varphi_i)$ required for a firm with core productivity φ_i to profitably operate in product h:

$$\pi_h\left(\varphi_i, \varphi_{ih}^*(\varphi_i)\right) = \frac{C_h P_h^{\sigma}}{\sigma}\left(\frac{\nu_h}{\rho\varphi_i\Phi_h\varphi_{ih}}\right)^{1-\sigma} - f_h = 0.$$

We now consider a firm's entry decision into the multiproduct environment. As the firm's draw of product-specific productivity is i.i.d. across products, expected profit is given by the integral over product categories $h \in [0, 1]$, net of a firm-level fixed cost f_i:

$$\pi(\varphi_i) = \int_0^1 \left[\int_{\varphi_{ih}^*(\varphi_i)}^{\infty} \pi_h(\varphi_i, \varphi_{ih})\, dG_h(\varphi_{ih})\right] dh - f_i. \tag{A.5}$$

Let M_h denote the measure of firms earning non-negative profits as determined by (A.5). For a given measure of potential entrants M_e, the measure of firms that operate in product h is

$$M_h = M_e \left(1 - G_i \left(\underline{\varphi}_i^h\right)\right),$$

where $\underline{\varphi}_i^h$ denotes the minimum firm-level productivity required to enter product category h.

The equilibrium measure of entrants M_e is determined by a free-entry condition. Denoting f_e as the entry cost, the expected profit across firm draws must equal the entry cost:

$$\int_{\varphi_i} \pi(\varphi_i)\, dG_i(\varphi_i) = f_e.$$

Emission Intensity and Aggregation

We now turn to the analysis of emissions for a given product category h, noting that all results generalize to any $h \in [0, 1]$. To aggregate firm-level outcomes, we follow the approach in Melitz (2003), expressing aggregate equilibrium variables in terms of a representative or "average" firm.

Define the revenue-weighted average productivity among operating firms in product h as:

$$\tilde{\varphi}^h = \left[\int_{\underline{\varphi}_i^h}^{\infty} \varphi^{\sigma-1} M_h\, dG_h(\varphi)\right]^{\frac{1}{\sigma-1}}. \tag{A.6}$$

Next, define aggregate emissions and aggregate output in product h as:

$$Z_h = \int_{\underline{\varphi}_i^h}^{\infty} z_{ih} M_h\, dG_h(\varphi), \tag{A.7}$$

$$Q_h = \left[\int_{\underline{\varphi}_i^h}^{\infty} q_{ih}^{\rho}(\varphi) M_h\, dG_h(\varphi)\right]^{1/\rho}, \tag{A.8}$$

where z_{ih} and q_{ih} denote firm-level emissions and output in product h. We consider two benchmark cases to characterize the aggregation of firm-level emission intensities at the product level.

In the first case, we assume a degenerate firm-product productivity distribution: $\varphi_{ih} = 1$ for all i and h, where Φ_h, as mentioned earlier, is a product-specific constant common across firms. Under this assumption, all firms with the same core productivity level have the same product-level productivity and we show that a firm's emission intensity exactly follows equation (1).

In the second case, we assume that product-level productivity φ_{ih} is drawn independently from a distribution $G_h(\varphi_{ih})$ that is independent of core productivity φ_i. This specification accommodates rich heterogeneity at the firm-product level while allowing for product-specific productivity—such as technological complexity—through the scaling factor Φ_h. We show that, in this setting, a firm's emission intensity follows equation (1) in expectation.

When the Firm-Product Level Productivity is Degenerate

We now formalize the relationship between aggregate and firm-level emission intensities in the case where firm-product-level productivity is degenerate. Specifically, we assume $\varphi_{ih} = 1$, so that product-level productivity is fully determined by the firm-level productivity φ_i and a product-specific scaling factor Φ_h.

The following proposition shows that, in this case, the aggregate (product-level) emission intensity coincides with that of a representative firm with average productivity $\tilde{\varphi}^h$.

Proposition 1. *When the firm-product-level productivity is degenerate, the aggregate emission intensity $\zeta_h \equiv Z_h/Q_h$ satisfies:*

$$\zeta_h = \zeta_{ih}(\tilde{\varphi}^h),$$

where $\zeta_{ih}(\tilde{\varphi}^h)$ denotes the firm-product-level emission intensity of a firm with productivity level $\tilde{\varphi}^h$ defined in equation (A.6).

Proof. For a firm with productivity φ_i, quantity and emissions are:

$$q(\varphi_i) = C_h P_h^\sigma \left(\frac{\nu_h}{\rho\varphi_i\Phi_h}\right)^{-\sigma},$$
$$z(\varphi_i) = C_h P_h^\sigma \cdot \frac{\alpha_h}{\tau}\left(\frac{\nu_h}{\rho\varphi_i\Phi_h}\right)^{1-\sigma}.$$

The emission intensity of a firm with productivity $\tilde{\varphi}^h$ is:

$$\zeta_{ih}(\tilde{\varphi}^h) = \frac{z(\tilde{\varphi}^h)}{q(\tilde{\varphi}^h)} = \frac{\alpha_h}{\tau} \cdot \frac{\nu_h}{\rho \tilde{\varphi}^h \Phi_h}.$$

Now consider aggregate emissions and output. After simple manipulation, it can be shown that Z_h and Q_h in equations (A.7) and (A.8) can be expressed as:

$$Z_h = C_h P_h^{\sigma} \cdot \frac{\alpha_h}{\tau} \left(\frac{\nu_h}{\rho} \right)^{1-\sigma} \left(\tilde{\varphi}^h \Phi_h \right)^{\sigma - 1},$$

$$Q_h = C_h P_h^{\sigma} \cdot \left(\frac{\nu_h}{\rho} \right) \left(\tilde{\varphi}^h \Phi_h \right)^{\sigma}.$$

It follows that the aggregate emission intensity is:

$$\zeta_h = \frac{Z_h}{Q_h} = \frac{\alpha_h}{\tau} \cdot \frac{\nu_h}{\rho \Phi_h} \cdot \frac{1}{\tilde{\varphi}^h} = \zeta_{ih}(\tilde{\varphi}^h). \tag{A.9}$$

□

The next result shows how the emission intensity of any firm i in product h relates to the aggregate product-level intensity.

Proposition 2. *The emission intensity of a firm with productivity φ_i is given by:*

$$\zeta_{ih}(\varphi_i) = \zeta_h \cdot \frac{\tilde{\varphi}^h}{\varphi_i}, \tag{A.10}$$

where the ratio $\tilde{\varphi}^h / \varphi_i$ can be interpreted as the firm-specific emission inefficiency factor, denoted by λ_i in equation (1).

Equation (A.9) can also be expressed as

$$\zeta_h = \frac{\alpha_h}{\rho \Phi_h} \cdot \frac{1}{\tilde{\varphi}^h} \cdot \left(\frac{w}{\tau} \right)^{1-\alpha_h},$$

and it suggests that PLEI decreases with average productivity of the firms that produce the product as well as policy stringency τ. In equation (A.10), firms only differ by their core productivity φ_i; however, if firms face different policy stringency τ_i, it will also be reflected as the difference in firm emission inefficiency factor, for instance as:

$$\zeta_{ih}(\varphi_i) = \zeta_h \cdot \frac{\tilde{\varphi}^h}{\varphi_i} \cdot \left(\frac{\tilde{\tau}^h}{\tau_i} \right)^{1-\alpha_h}, \tag{A.11}$$

where $\zeta_h = \frac{\alpha_h}{\rho \Phi_h} \cdot \frac{1}{\tilde{\varphi}^h} \cdot \left(\frac{w}{\tilde{\tau}^h}\right)^{1-\alpha_h}$ and $\tilde{\tau}^h$ captures the average regulatory stringency for firms that produce product h.

When Firms Draw Product-Level Productivity Independently

We now consider the case where firms draw their product-level productivity φ_{ih} independently from a distribution $G_h(\varphi_{ih})$, which is assumed to be independent of the firm-level productivity φ_i. In this setting, the aggregate emission intensity ζ_h can still be related to the firm-product-level emission intensity via a tractable expression.

Specifically, the emission intensity of a firm-product pair $(\varphi_i, \varphi_{ih})$ can be expressed as:

$$\zeta_{ih}(\varphi_i, \varphi_{ih}) = \zeta_h \cdot \frac{\tilde{\varphi}^h}{\varphi_i \varphi_{ih}}. \tag{A.12}$$

To characterize firm-product-level emission intensity, we assume $\mathbb{E}[\varphi_{ih}^{-1}] = 1$, which is equivalent to normalizing the unit labor requirement.

Proposition 3. *Suppose that the firm-product-level productivity φ_{ih} is independent of firm-level productivity φ_i and satisfies $\mathbb{E}[\varphi_{ih}^{-1}] = 1$. Then, the expected firm-product emission intensity conditional on φ_i satisfies:*

$$\mathbb{E}\left[\zeta_{ih}(\varphi_i, \varphi_{ih}) \mid \varphi_i\right] = \zeta_h \cdot \frac{\tilde{\varphi}^h}{\varphi_i}. \tag{A.13}$$

Proposition 3 implies that the expected emission intensity of a firm-product pair is proportional to the product-level average emission intensity ζ_h, scaled by the firm inefficiency factor $\frac{\tilde{\varphi}^h}{\varphi_i}$. Thus, even when firm-product productivity is idiosyncratically drawn, one can still recover an empirical expression similar to equation (1) in expectation.

This relationship implies that consistent estimation of PLEI is attainable under independent firm-product-level productivity draws, particularly as the number of observations increases. We demonstrate this numerically in the Monte Carlo simulations below.

Monte Carlo Simulation

In this section, we use Monte Carlo exercises to illustrate that, under our framework, firm-product-level productivity shocks are mean-zero and uncorrelated, effectively behaving as classical white noise. As such, assuming (A.10) introduces no bias in expectation, given that equation (A.13) holds on average.

In the first experiment, we numerically verify equation (A.13). We compute $\zeta_{ih}(\varphi_i, \varphi_{ih})$ and $\zeta_{ih}(\varphi_i)$, then plot the sample mean of their ratio, along with 95% confidence intervals, across varying numbers of firms in Figure A.1.[36] As the number of firms increases, the mean of $\zeta_{ih}(\varphi_i, \varphi_{ih})$ converges to $\zeta_{ih}(\varphi_i)$, consistent with the intuition that firm-product-level idiosyncrasies are averaged out in large samples.

Figure A.2 further corroborates this pattern. Using our iteration algorithm, we simulate multi-product firms across different sample sizes.[37] For each specification, we conduct 201 independent Monte Carlo simulations and report the bootstrap distribution of the percentage differences in ζ_h estimates generated with and without firm-product-level productivity shocks. The distribution narrows markedly as the number of firms increases, reinforcing the interpretation of these shocks as white noise. These results provide empirical support for treating the PLEI structure in equation (A.13) as a valid approximation in our context.

[36] The data generating process simulates firm-level output and emissions for varying numbers of firms (F). For each F, firm productivity is drawn from a Pareto distribution with shape parameter $\theta = 6$ and scale $b = 1$, while idiosyncratic productivity shocks are sampled from a log-normal distribution with mean $\mu = 0.125$ and standard deviation $\sigma = 0.5$. The model considers a single product and sets demand elasticity to $\sigma = 3$. Emission intensities are computed for each firm both with and without idiosyncratic shocks according to equations (A.12) and (A.10), respectively.

[37] The data generating process simulates firm-level output and emissions for different numbers of firms (F). For each F, firm productivity is drawn from a Pareto distribution with shape parameter $\theta = 6$ and scale $b = 1$. Idiosyncratic productivity shocks are sampled from a log-normal distribution with mean $\mu = \sigma^2/2$ and standard deviation $\sigma = 0.001$. The model considers $H = 7$ products and sets demand elasticity to $\sigma = 3$. For each firm and product, output and emissions are computed both with and without idiosyncratic shocks. PLEI are then calculated for each case using our iterative algorithm. The percent difference in emission intensities between the idiosyncratic and baseline cases is bootstrapped to construct confidence intervals.

Figure A.1: Mean Estimates of Firm-Product Level Emission Intensity

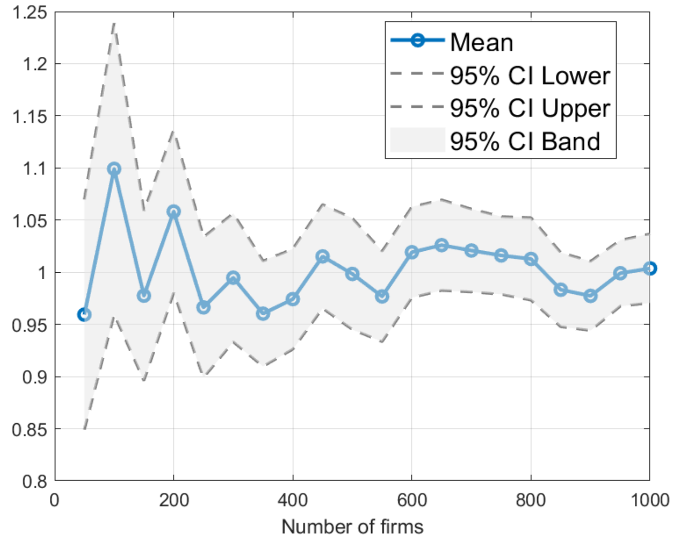

Notes: This figure reports the mean estimates and 95% confidence intervals for the ratio $\zeta_{ih}(\varphi_i, \varphi_{ih})/\zeta_{ih}(\varphi_i)$, reflecting firm-product-level heterogeneity. The true emission intensity follows equation (A.12), while the estimand corresponds to the ratio between equations (A.10) and (A.12).

Figure A.2: Bootstrap Distribution of the Estimates of ζ_h

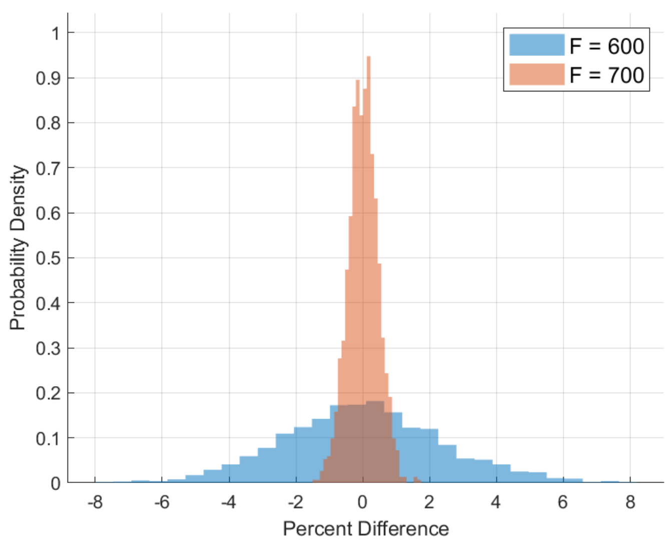

Notes: This figure displays the bootstrap distribution of the percentage differences in ζ_h estimates generated with and without firm-product-level productivity shocks. The dispersion narrows significantly as the number of firms increases, supporting the interpretation of firm-product-level productivity shocks as white noise.

B Monte Carlo Simulation for PLEI

To assess the performance of our iterative algorithm, we employ a Monte Carlo (MC) simulation approach. For simplicity, without loss of generality, we choose a single emission category, COD, as our reference pollutant for simulation. The data generating process (DGP) is carefully designed to reflect the key statistical moments of our firm-product level data.

Our simulation serves two core purposes. First, we investigate our algorithm's performance when the DGP deviates from the assumption of a uniform emission inefficiency parameter λ_i across all products within a given firm. This evaluation is achieved by comparing the outcome under two distinct DGPs. The first DGP aligns with our model's assumption, with an inefficiency parameter λ_i that varies only across firms. The second DGP permits λ_{hi} to vary across both firms and their respective products. This design offers insights into the robustness of our algorithm in the face of product-level emission inefficiency variation within firms. Second, we rely on MC simulations to demonstrate that our iteration method outperforms ordinary least squares (OLS) in estimating PLEI.

B.1 Data Generating Process

As mentioned in Section 2.1, our firm-product level data combines three sources: the China's Environmental Statistical Database, the Annual Survey of Industry, and Chinese customs data. This final dataset encompasses 569,397 firms and spans 5,024 unique products. To streamline the simulations, we constrain the sample of each simulated dataset to 10,000 firms and cap the product count at 90, ensuring a comparable firm-product ratio (calculated as $90 \approx 10\,000 \times 5024/569\,397$).

The benchmark estimates from Section 2.2 serve as the true ζ_h values in our Monte Carlo simulation. We note that (i) a substantial proportion (50.6%) of our ζ_h estimates are zero, (ii) the distribution of ζ_h is densely packed around positive yet tiny values, and

(iii) a handful of sizable ζ_h values skew the distribution rightward. Based on the first two observations, in our Monte Carlo simulations, we assume that 70% of products have zero emission intensities. This accounts for the 50.6% products with exactly zero emissions, plus approximately 20% of products whose ζ_h values can be considered effectively zero ($\zeta_h < 1 \times 10^{-7}$).

To start, we categorize products with ζ_h values over the 70th percentile value into 27 evenly distributed product groups based on their emission intensity. This product group count is derived by multiplying the number of products in our simulation (90) by the proportion of products with positive emission intensity (30%). For products not exceeding the 70th percentile threshold, we shuffle them randomly and segment them into 63 uniform groups. This correspondence between the simulated 90 product groups and the original 5,024 products remains invariant across all simulation datasets. As detailed in Appendix B.2, this approach aptly preserves the distribution of ζ_h.

In our Monte Carlo analysis, we label the 27 product groups with positive ζ_h as "dirty," while the rest are termed "clean". This definition of being "dirty" is slightly different from the top 10% emission-intensive products used in the main text. For each of the "dirty" product groups, the median ζ_h value from the corresponding original products is used across all simulations. The emission intensities for all "clean" products are set to zero.

Next, we detail the firm sampling methodology, which aims to preserve the quantity distribution of products each firm produces. In our raw data, 94.46% of firms produce ten or fewer products. After aggregating the original products into 90 distinct groups, we observe that 94.73% of firms still produce ten or fewer such product groups. By construction, the latter percentage is higher than the former, but the striking similarity in percentages can be attributed to the highly skewed distribution of products per firm. Namely, firms that produce hundreds of HS 6-digit products are also involved with more than ten product groups, hence aligning the two percentages. In the subsequent discussion, we use the terms "product" and "product group" interchangeably , with the ζ_h values of these groups designated as the "true" ζ_h values for the simulation.

For firm sampling, while preserving the distribution of product counts, we randomly choose firms with replacement from our full dataset. Upon selecting a firm, a simulated counterpart is created, replicating its product count and corresponding output values (y_{hi}). Thus, the firms in our Monte Carlo simulation, though fewer in number, have the similar distribution of product counts and and quantities as the original data.

For our first set of Monte Carlo simulations, referred to as DGP-1, the inefficiency parameter λ_i is designed to vary across firms but remains invariant across all products within a firm. This ensures that the emissions at the product level (h) for a specific firm i can be expressed as $z_{hi} = y_{hi}\zeta_h\lambda_i$. For dirty products where $\zeta_h > 0$, the parameter λ_i must implicitly conform to the following equation[38]

$$\sum_i y_{hi}\lambda_i = \sum_i y_{hi}, \quad \forall h. \tag{B.1}$$

Given the substantially larger number of firms relative to products, multiple potential solutions for λ_i can satisfy equation (B.1). Consequently, we utilize the empirical distribution to set constraints on the λ_i values during simulations. In particular, we curtail both the top and bottom 20% of the empirical λ_i distribution to eliminate outliers and then impose that the solution set for λ_i to equation (B.1) must match the minimum, maximum, and mean of this trimmed distribution.

Having determined, ζ_h, y_{hi} and λ_i, firm-product emissions are calculated as $z_{hi} = y_{hi}\zeta_h\lambda_i$. We then posit that emission data are observed with firm-specific noise, denoted by ϵ_i. Thus, the observed emission at the firm level is expressed as $z_i = (1+\epsilon_i)\sum_h z_{hi}$. Taking a conservative stance, we assume that ϵ_i is drawn from a uniform distribution ranging from -30% to 30%.

In the second data generating process, referred to as DGP-2, we let λ_{hi} to be more flexible to exhibit variability not just across both firms and products within each firm.

[38]To see this, express the emission intensity as $\left(\zeta_h = \frac{\sum_i y_{hi}\zeta_h\lambda_i}{\sum_i y_{hi}}\right)$, where the numerator and the denominator respectively indicate total emissions and output associated with product h. By realigning the denominator to the left and negating mutual ζ_h values, equation (B.1) is derived.

The counterpart to equation (B.1) can be formulated as:

$$\sum_i y_{hi}\lambda_{hi} = \sum_i y_{hi}, \quad \forall h. \tag{B.2}$$

For each simulation under DGP-2, we determine a set of λ_{hi} satisfying equation (B.2). This process retains the minimum, maximum, and mean values associated with λ_i, highlighting the nuances of within-firm and between-product emission intensity variations. It is noteworthy that a uniform λ_{hi} across all products within a firm simplifies to the specific case of λ_i described in equation (B.1).

Given this setup, the emission value of product h from firm i can be expressed as $z_{hi} = y_{hi}\zeta_h\lambda_{hi}$. As in DGP-1, we then introduce firm-specific measurement error by applying a random shock, drawn from a uniform distribution between -30% and 30%, to the total firm-level emissions, z_i.

For each DGP, we generate 500 simulated datasets. The iterative algorithm is initialized with $\zeta_h = 1$ for all products. For robustness checks, we also explored other starting values for ζ_h, chosen randomly from [0.1, 5]. The results remained highly robust to the choice of initial value.

B.2 Comparison Between Actual and Simulated Datasets

To ensure the empirical relevance of our simulations, we generate our simulated data that reflect the empirical distributions of firm-product level output and product-specific emission intensities. The stochastic nature of the simulation arises from three sources: the random sampling of firms, the determination of the inefficiency parameters (λ_i or λ_{hi}), and the introduction of measurement errors. In this section, we validate our approach by comparing key moments from the actual and simulated datasets.

Figure B.1 compares the distribution of firm-product level output from the original dataset against the simulated data, showing values from the 1st to the 99th percentile. Since both DGP-1 and DGP-2 use the same output generation process, the figure shows only the results for DGP-1 for brevity. The close alignment between the percentile val-

Figure B.1: Firm-Product Level Output Values

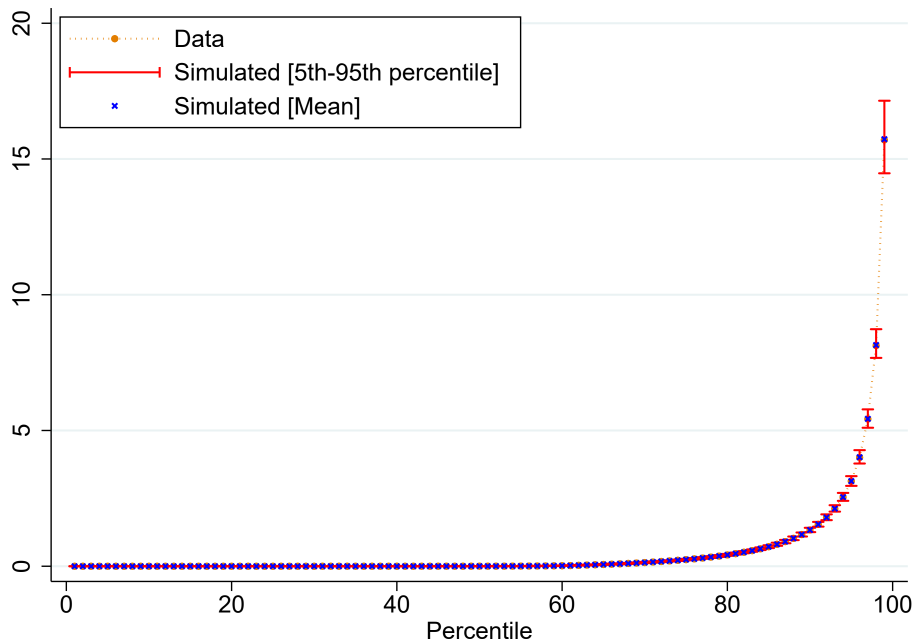

Notes: This figure compares the distribution of firm-product level output in our original dataset with results from 500 simulations. The dots represent the actual output values at each percentile (from 1 to 99) in our data. The corresponding results from the simulations are summarized by the mean value at each percentile, as well as the range between the 5th and 95th percentiles across all 500 runs.

ues of the actual and simulated data validates our methodology. Specifically, for each percentile, the mean of the simulated values lies within one standard deviation of the corresponding value from the actual data.

Next, we provide a comparison focusing on firm-product level emissions. Because emissions are not directly observed at this level of granularity for multi-product firms, we infer these values for the "actual" data using our empirical estimates of ζ_h and λ_i. As presented in Figure B.2, there is a strong alignment between these inferred actual emissions and the simulated emissions under both DGPs. This result confirms that our data generating processes effectively replicate the essential features of the emission data.

Figure B.2: Firm-Product Level Emissions

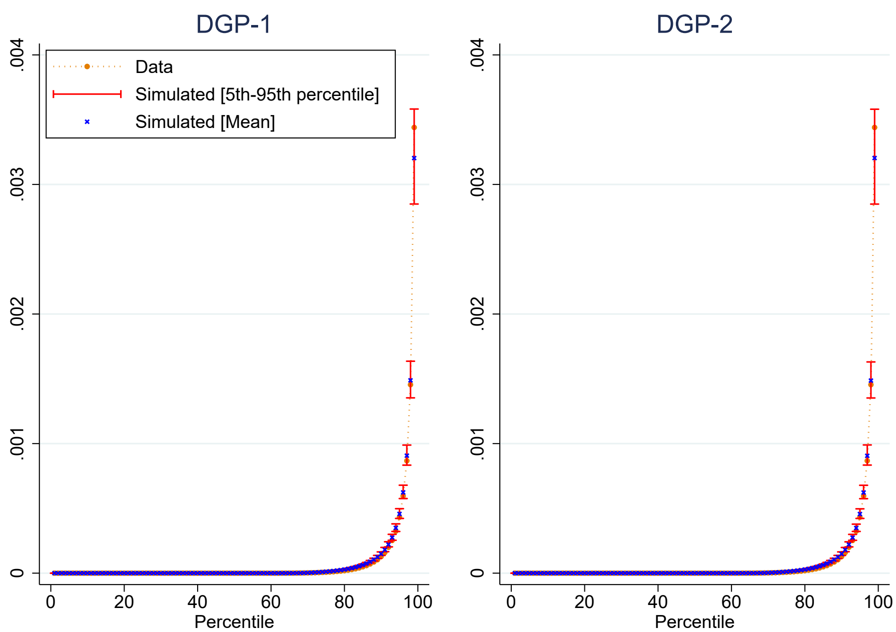

Notes: This figure compares the distribution of firm-product level emissions in our original dataset with results from 500 simulations. The dots represent the inferred actual emission values at each percentile (from 1 to 99) in our data. The corresponding results from the simulations are summarized by the mean value at each percentile, as well as the range between the 5th and 95th percentiles across all 500 runs. DGP-1 refers to the data generating process where λ_i varies only across firms, while DGP-2 refers to the process where λ_{hi} varies across both firms and products.

B.3 DGP-1: λ_i Varies Across Firms

Utilizing our iterative algorithm, we compute ζ_h for each of the 500 simulated datasets. In the left panel of Figure B.3, we display a scatter plot comparing the estimated and true ζ_h values on a logarithmic scale. For each product, the figure depicts the median estimate across all 500 simulations, along with the range spanning the 5th to the 95th percentiles. To visualize products with zero true emissions ("clean products") on a logarithmic scale, we add a small constant (half the smallest positive true ζ_h value) to both the true and estimated values before taking the logarithm.

As shown in in the left panel of Figure B.3, the strong alignment of the estimated values with the 45-degree line suggests that our algorithm consistently and accurately recovers the true ζ_h values. This visual evidence is supported by the statistics presented in the figure: the mean and median correlation coefficients between the estimated and true values (calculated before log transformation) both exceed 0.998.

B.4 DGP-2: λ_{hi} Varies Across Firms and Products

In DGP-2, we introduce a additional layer of complexity by allowing the true inefficiency parameter, λ_{hi}, to differ across products within a given firm. This added variation, which is not explicitly addressed by our iteration algorithm, introduces further intricacies to our PLEI estimates beyond the inherent measurement error. Under this DGP, we still perform our iteration under the maintained assumption that the inefficiency parameter varies only at the firm level. The purpose is to assess the ramification of our assumption when it does not fully align with the true data generating process.

The results for DGP-2 are presented in the right panel of Figure B.3. Compared to DGP-1, there is a marginal decline in the correlation coefficients between the estimated and true ζ_h values. However, their mean and median remain prominently above 0.998. For some products, we also observe a slight widening of the 5th-to-95th percentile range,

Figure B.3: Monte Carlo Results

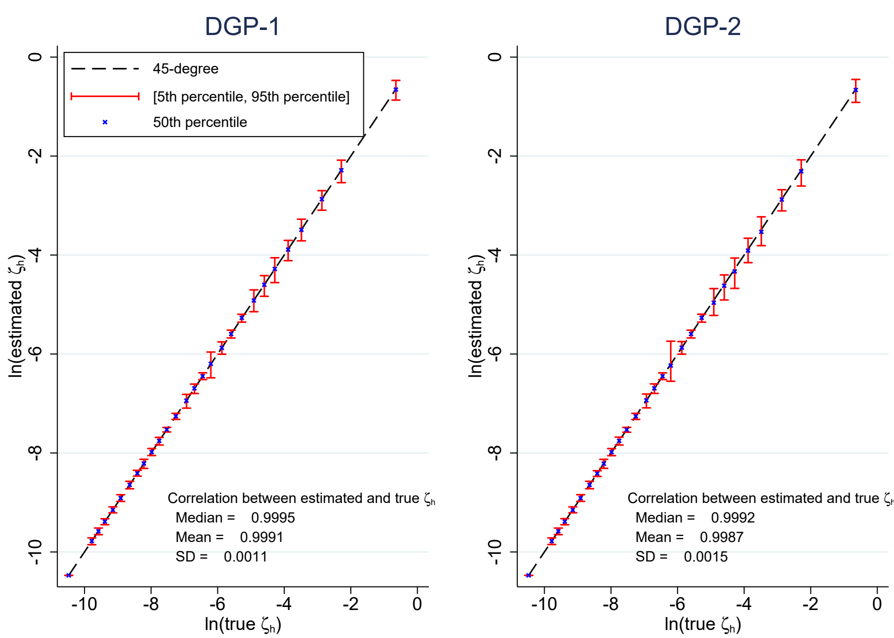

Notes: The panels in this figure show the performance of our iterative algorithm in estimating ζ_h under DGP-1 and DGP-2. Each panel compares the true ζ_h values against estimates from the simulations. We focus on the logarithm of median estimate for each product, with the range from the 5th to 95th percentile derived from 500 simulations. For clean products, we augment both the estimated and true ζ_h values by adding half the smallest positive value from the true ζ_h of dirty products before the log transformation. The bottom-right of each panel reports the mean, median, and standard deviation of the correlation coefficients between the estimated and true ζ_h values.

which indicates a minor loss of estimation efficiency. Nevertheless, the estimates remain closely aligned with the 45-degree line, demonstrating that our algorithm is robust to this form of unmodeled, intra-firm heterogeneity in λ_{hi}.

B.5 Regression Approach

One potential strategy to estimate ζ_h is to employ ordinary least squares (OLS) using the following model specification:

$$z_i = \sum_h y_{hi}\zeta_h + e_i. \tag{B.3}$$

In this equation, e_i represents the error term, and ζ_h can be interpreted as the PLEI. While the computational efficiency of OLS might be an advantage given its speed relative to our iterative approach, it is inherent with certain limitations. Primarily, equation (B.3) relies on e_i to encompass the firm efficiency parameter in an additive fashion. This suggests that a firm would still have emissions equal to e_i even with zero production, a feature inconsistent with the underlying physical process. Second, OLS is not constrained to produce non-negative estimates for ζ_h, meaning it can paradoxically suggest that production reduces emissions.

We evaluate the performance of OLS by applying it to the same simulated datasets from DGP-1 and DGP-2. The results are illustrated in Figure B.4, with panels corresponding to each DGP. It is immediately apparent from the left panel (DGP-1) that the OLS estimates are less accurate than those from our iterative method. The mean correlation coefficient between the OLS estimates and the true ζ_h values is substantially lower. More tellingly, the standard deviation of these correlation coefficients surges from 0.0011 (iteration method) to 0.2208 (OLS), highlighting the superior stability and accuracy of our iterative method in calculating PLEI.

Moreover, a significant fraction of OLS estimates (46.80%) are negative. As a result, we cannot plot the estimates on the log-log scale employed in Figure B.3. For clarity, only

Figure B.4: Monte Carlo Results (Ordinary Least Squares)

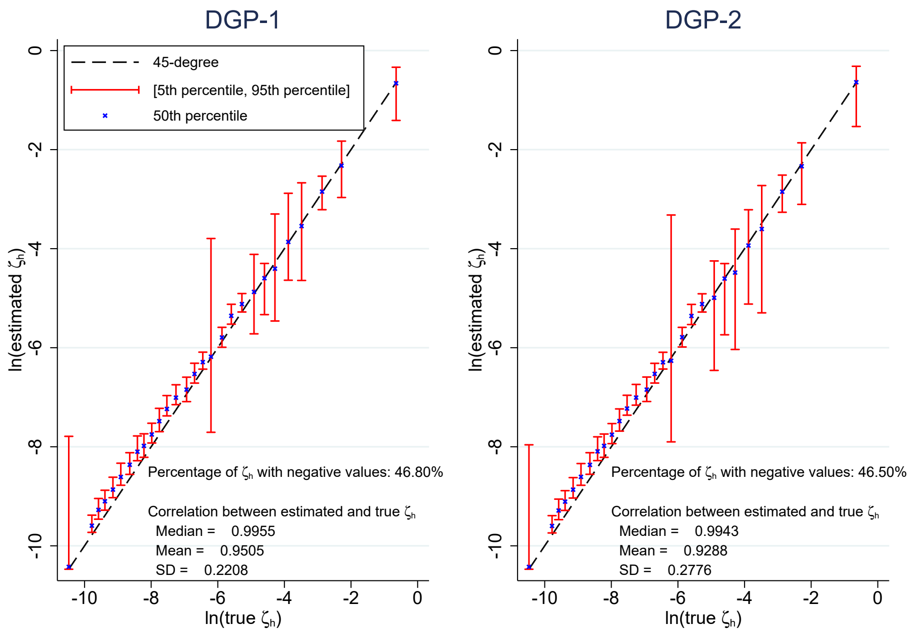

Notes: The panels in this figure display the ζ_h values estimated using OLS for DGP-1 (left) and DGP-2 (right). Each panel plots the logarithm of median values against the true values for each product, along with the span between the 5th and 95th percentile derived from 500 simulations. For clean products, we augment both the estimated and true ζ_h values by adding half the smallest positive value from the true ζ_h of dirty products before the log transformation. Negative ζ_h estimates produced by OLS are excluded from the plots. The bottom-right of each panel reports the mean, median, and standard deviation of the correlation coefficients between the estimated and true ζ_h values.

non-negative OLS estimates are plotted in Figure B.4. Compared with the left panel of Figure B.3, the median OLS estimates deviate more noticeably from the 45-degree line. Additionally, the variation – measured by the span between the 5th and 95th percentiles – is substantially greater under the OLS method compared to our iterative method. This underscores the superior precision and reliability of our iterative approach, particularly within the non-negative domain. The results under DGP-2, shown in the right panel of Figure B.4, lead to the same conclusions.

To provide a quantitative comparison between our iteration algorithm and OLS, we compute the mean absolute errors (MAE) for *clean* products and mean absolute percent-

Table B.1: Mean Error Comparison between Iteration and OLS

Clean Products		
	MAE^{ITER}	MAE^{OLS}
DGP-1	8.101E-07	2.858E-04
DGP-2	7.268E-07	2.776E-04
Dirty Products		
	$MAPE^{ITER}$	$MAPE^{OLS}$
DGP-1	0.0610	0.4126
DGP-2	0.0750	0.4584

Notes: For clean and dirty products, we report the mean absolute errors (MAE) and the mean absolute percentage errors ($MAPE$) between the estimated and true ζ_h, respectively. $ITER$ and OLS indicate our iteration algorithm and OLS, respectively.

age errors ($MAPE$) for *dirty* products. The MAE^j is given by:

$$MAE^j = \frac{1}{N \cdot H_c} \sum_n \sum_h \left| \zeta_h^{true} - \zeta_h^{j,n} \right|,$$

where n indexes a simulated dataset, N denotes the total number of simulations, H_c represents the number of clean products, j denotes the estimation method ($ITER$ or OLS), and $\zeta_h^{true} = 0$ for clean products. For *dirty* products, $MAPE^j$ is described as:

$$MAPE^j = \frac{1}{N \cdot H_d} \sum_n \sum_h \left| \frac{\zeta_h^{true} - \zeta_h^{j,n}}{\zeta_h^{true}} \right|,$$

where H_d denotes the number of dirty products. While $MAPE$ is more intuitive than MAE, its computation requires a non-zero denominator ζ_h^{true}, making it unsuitable for clean products.

Table B.1 presents the MAE and $MAPE$ outcomes. For clean products, the iteration method yields an MAE that is nearly two orders of magnitude lower than that of OLS. For dirty products, the $MAPE$ for the iterative method is approximately 16% of the OLS value. These findings further demonstrate the precision of our iterative approach in estimating ζ_h.

C Verifying PLEI with External Datasets

In addition to the CESD, various datasets report on China's industrial emissions and their intensities. Primary sources include China Statistical Yearbook and China Statistical Yearbook on Environment from the National Bureau of Statistics (SYB). These yearbooks disclose annual emissions for various pollutants, which include NO_x, SO_2, soot and dust, ammoniacal nitrogen, and COD, classified under the CIC 2-digit level. Additionally, the Eora Global Supply Chain Database (EORA) and EXIOBASE (EXIO), both of which are multi-region environmentally extended input-output (IO) tables, also include sectoral level emissions and output data, although each dataset has its own distinct sectoral classifications.

Comparing our PLEI calculations to emission intensities from these alternative sources is not straightforward. One major complication is the inconsistent emission categories reported in different datasets. For our pollutant types, we associate them with the same or nearest emissions accounts, ensuring a reasonable comparison.[39] A further challenge emerges from the distinct industrial identifiers each dataset deploys. To ensure consistency during cross-comparison, we aggregate emission intensity measures across all sources to the CIC 2-digit level, the broadest classification shared by the datasets.

Figures C.1 through C.3 offer a bilateral comparison of emission intensity estimates across datasets. Broadly speaking, our PLEI-derived industry-level emission intensities exhibit strong correlations with those derived from other sources. All observed correlations are positive, with the majority surpassing 0.5. The strongest correlation emerges between PLEI and SYB estimates. For comparisons involving EORA and EXIO, discrepancies are more pronounced, potentially attributable to discrepancies in pollutant classifi-

[39] For example, CO_2 emissions used in our PLEI computation stem from reported corporate fossil fuel utilization. In contrast, the closest measure EORA provides, termed "Fuel Combustion Activities (PRIMAP—CO2—IPC1A—Gg)", spans only a segment of sectors. This leads us to adopt data tagged as "National Total excluding LULUCF (PRIMAP—CO2—TOTALexcludingLULUCF—Gg)", not ideally aligned with our PLEI metric.

cations, industry identifiers, or the intrinsic quality of the EORA/EXIO datasets.[40] Nevertheless, the robust correlation observed for specific emission categories (like Ammoniacal Nitrogen, Dust, and SO_2 in the PLEI vs. EORA comparison, and Dust in the PLEI vs. EXIO analysis) reinforces the efficacy of our PLEI estimates in gauging the environmental impact of industrial production.

[40]The creation of the multi-region input-output table necessitates reliance on sectorial or regional growth rates to infer certain emission account data, such as those related to land-use changes and deforestation.

Figure C.1: The Comparison of Emission Intensity Estimates: PLEI vs. SYB

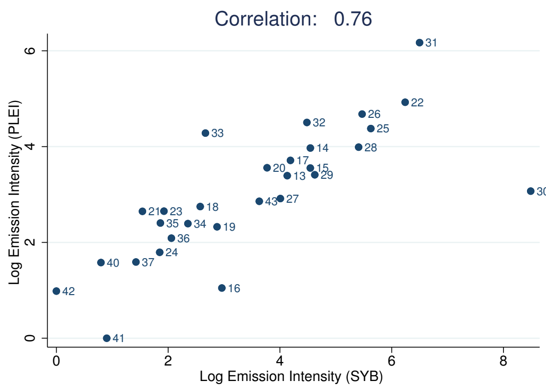

(a) NO_x

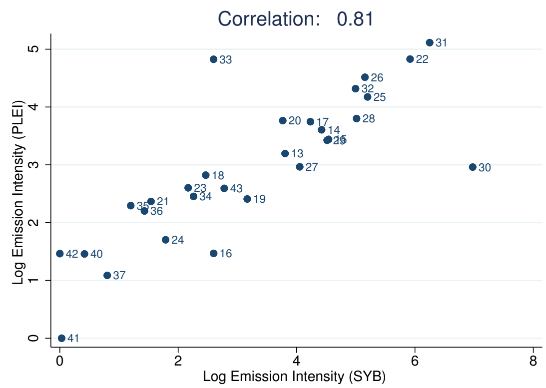

(b) SO_2

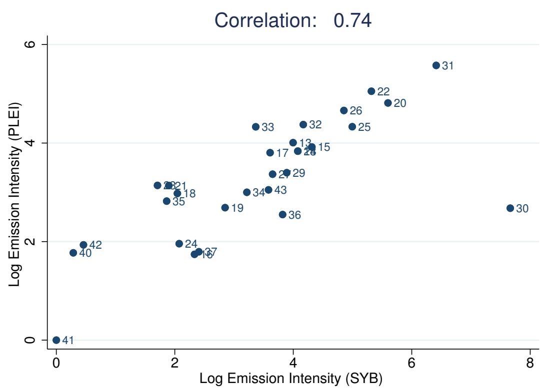

(c) Soot

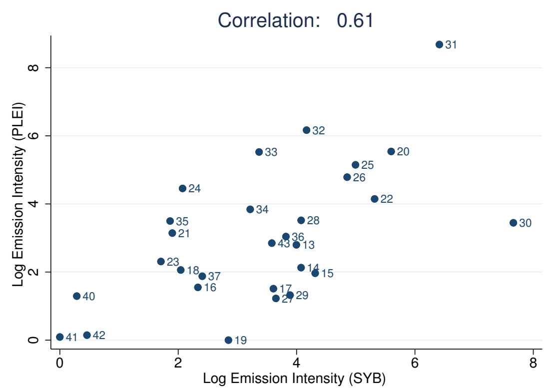

(d) Dust

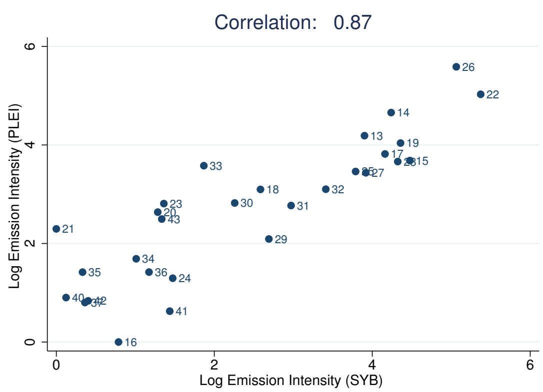

(e) Amm. Nit.

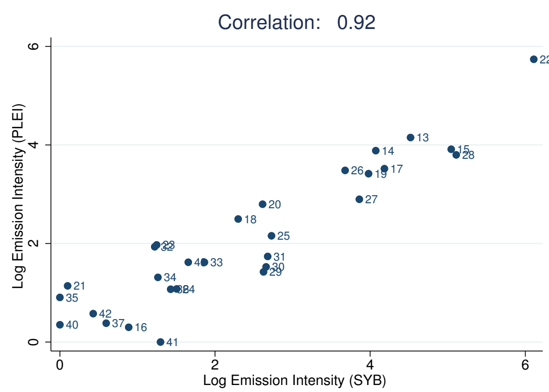

(f) COD

Notes: These figures illustrate the bilateral comparison of emission intensity estimates between PLEI and SYB, standardized to the CIC 2-digit categorization. Each subfigure's title shows the specific pollutant under analysis. Each dot represents the paired estimates of emission intensities for a specific CIC 2-digit industry, with the industry code displayed next to the dot. The x-axis showcases the logarithmic values of emission intensities sourced from SYB data, while the y-axis depicts the logarithmic values derived from PLEI assessments. The correlation coefficient between these two estimation sets is displayed at the top of each subfigure.

Figure C.2: The Comparison of Emission Intensity Estimates: PLEI vs. EORA

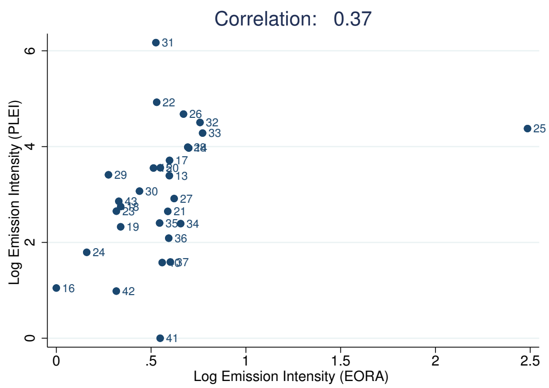

(a) NO_x

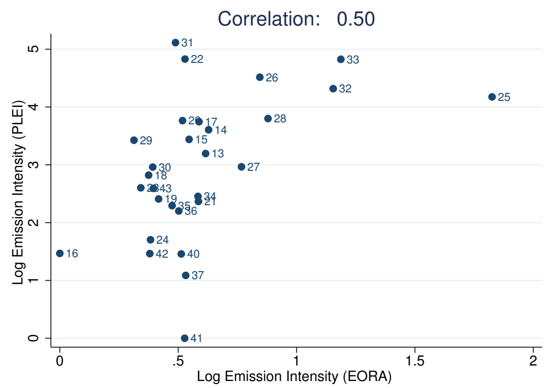

(b) SO_2

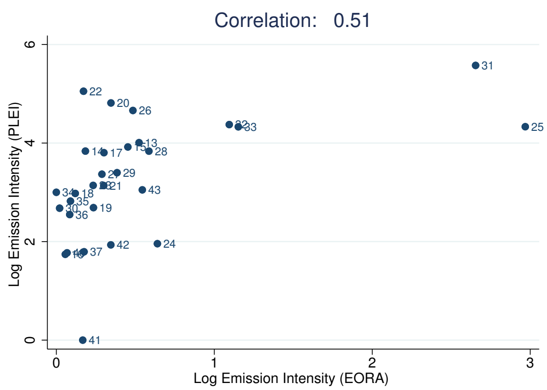

(c) Soot

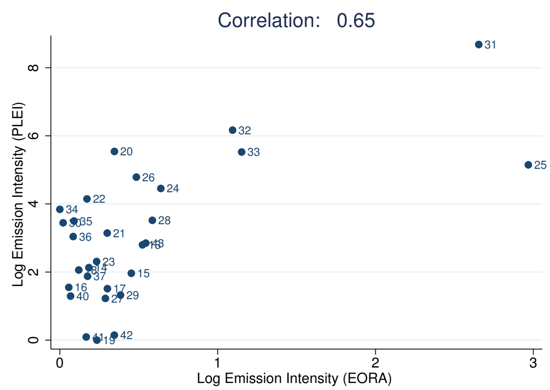

(d) Dust

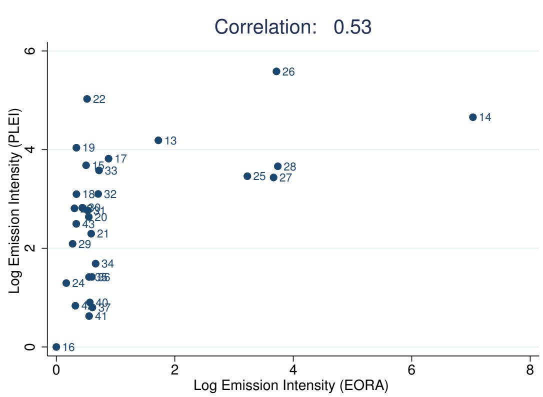

(e) Amm. Nit.

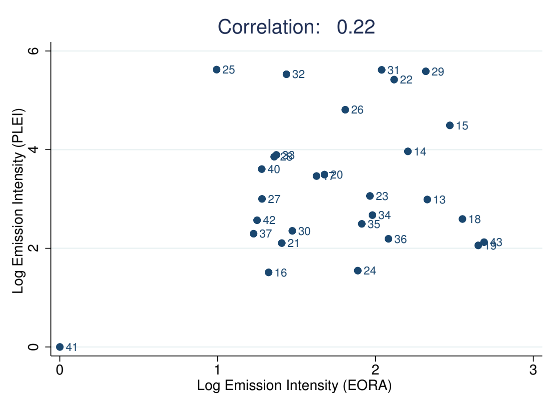

(f) CO_2

Notes: These figures illustrate the bilateral comparison of emission intensity estimates between PLEI and EORA, standardized to the CIC 2-digit categorization. Each subfigure's title shows the specific pollutant under analysis. Each dot represents the paired estimates of emission intensities for a specific CIC 2-digit industry, with the industry code displayed next to the dot. The x-axis showcases the logarithmic values of emission intensities sourced from EORA data, while the y-axis depicts the logarithmic values derived from PLEI assessments. The correlation coefficient between these two estimation sets is displayed at the top of each subfigure.

Figure C.3: The Comparison of Emission Intensity Estimates: PLEI vs. EXIO

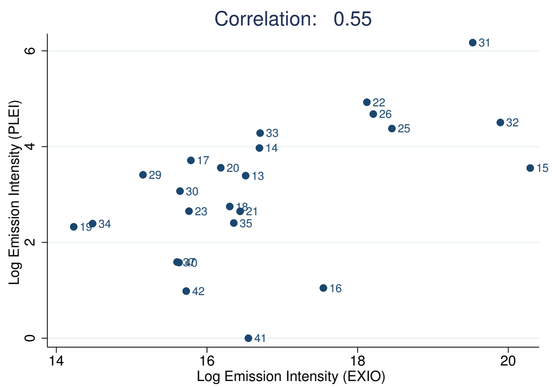

(a) NO_x

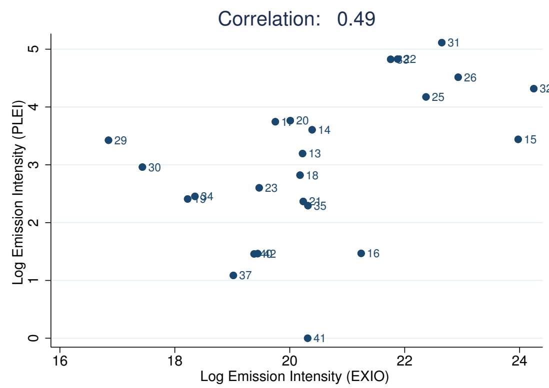

(b) SO_2

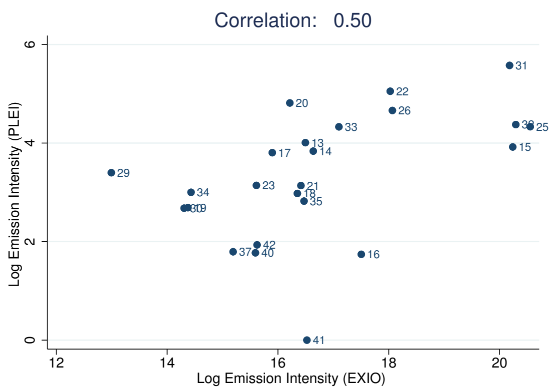

(c) Soot

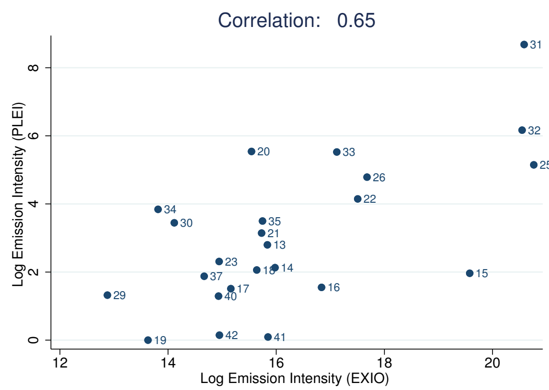

(d) Dust

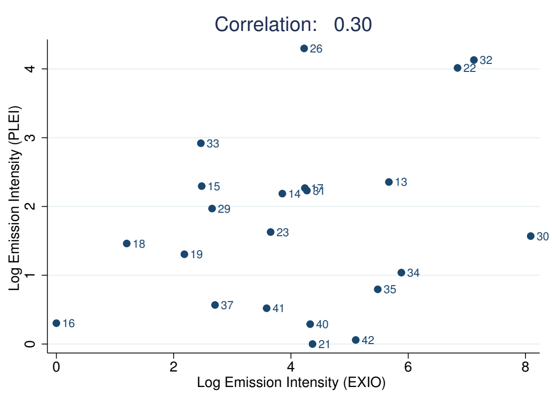

(e) Water

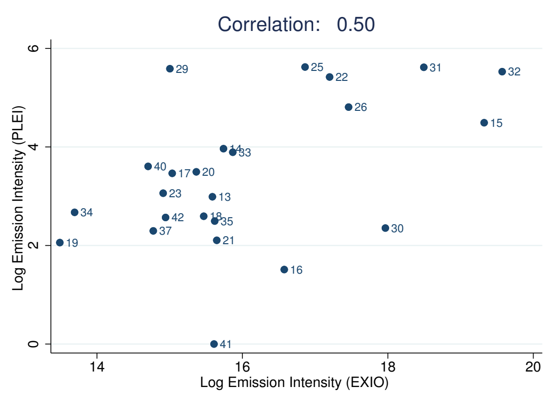

(f) CO_2

Notes: These figures illustrate the bilateral comparison of emission intensity estimates between PLEI and EXIO, standardized to the CIC 2-digit categorization. Each subfigure's title shows the specific pollutant under analysis. Each dot represents the paired estimates of emission intensities for a specific CIC 2-digit industry, with the industry code displayed next to the dot. The x-axis showcases the logarithmic values of emission intensities sourced from EXIO data, while the y-axis depicts the logarithmic values derived from PLEI assessments. The correlation coefficient between these two estimation sets is displayed at the top of each subfigure.

D Cross-Country Comparison of Industrial-Level Emission Intensities

In this subsection, we employ EXIO to investigate the correlation of industrial-level emission intensities between China and its trade partners. Our empirical analysis utilizes the PLEI measure, derived from Chinese manufacturing data, to identify products with high pollution levels in both export and domestic sectors. This methodology inherently presumes a high degree of consistency in the ranking of emission intensities across different countries. Leveraging the multi-regional IO table of EXIO, which provides output and emissions data for 162 industries across 48 countries, we calculate the pairwise rank correlation of emission intensities at the industrial level between China and each of the other 47 countries, focusing on the pollutants measured by the PLEI.

Figure D.1 presents the box plots illustrating the pairwise rank correlations for the six pollutants. The box plots reveal that the majority of these correlations surpass 0.6, indicating a strong level of consistency in the ranking of industrial emission intensities between China and other countries. This finding underscores the reliability of our empirical examination using PLEI.

Figure D.1: Cross-National Comparison of Industrial-Level Emission Intensities

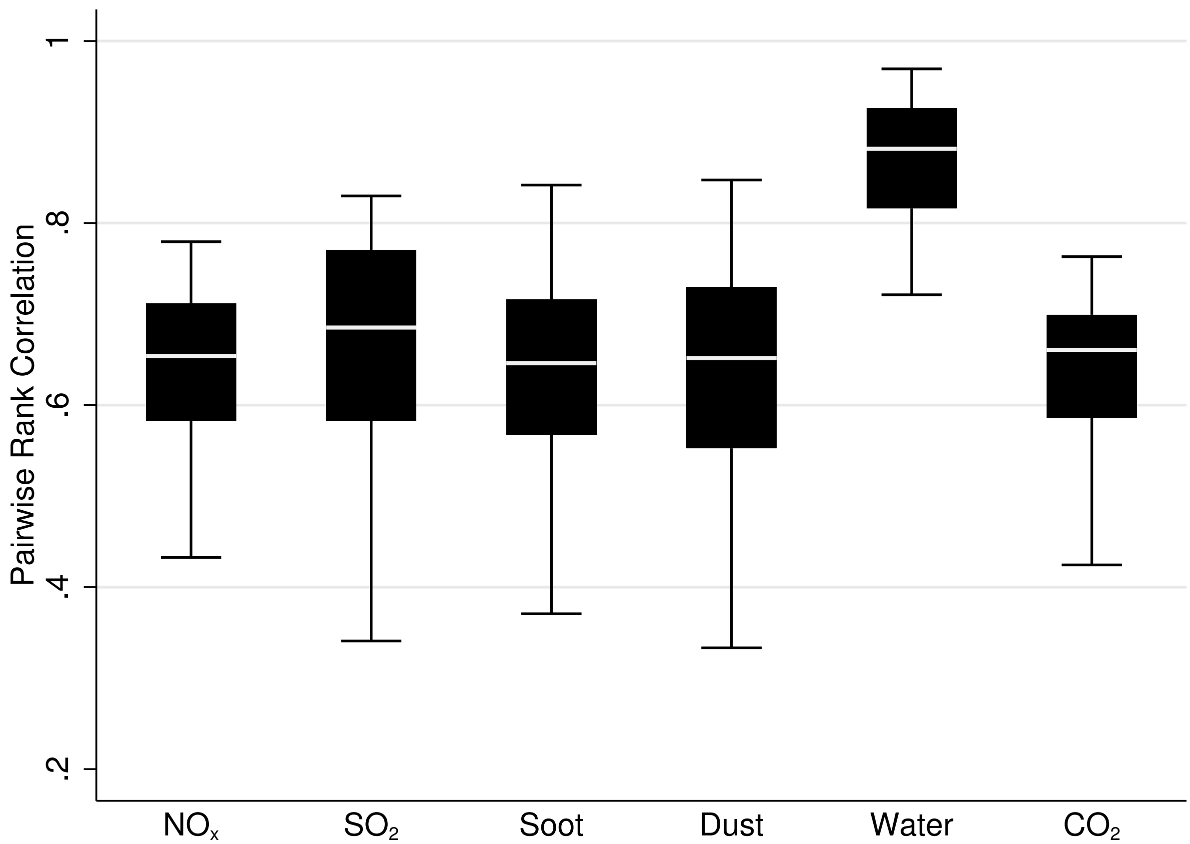

Notes: This figure displays box plots of the pairwise rank correlation of emission intensities between China and other countries for six pollutants calculated using EXIO. The horizontal axis indicates the type of pollutant. The vertical axis shows the value of rank correlation.

E Time Consistency of ζ_h

We operate under the presumption that PLEI reflect the time-invariant production attributes of each product. This subsection rigorously probes this hypothesis. A naïve method involves calculating emission intensities, denoted as $\{\zeta_{ht}\}$, separately for each year. Yet, this strategy encounters two problems. First, a large amount of firm-level observation for individual products is needed for a precise PLEI calculation. Utilizing a single year's data exacerbates the likelihood of encountering products manufactured predominantly by few firms, thereby making it difficult to disentangle the differentiation between product-specific and firm-specific attributes. The subsequent, and arguably more pressing issue, arises when $\{\lambda_{it}\}$ calculated from this strategy loses inter-temporal comparability. Specifically, within our algorithm, if a firm witnesses a 10% increase in λ_{it} in a given year, it signals a commensurate increase in emission intensities for its entire product portfolio, both when compared across firms and compared with other years. Such interpretation becomes untenable when $\{\zeta_{ht}\}$ is calculated distinctively for each year.

Intuitively, when $\zeta_{ht} = \zeta_{h(t-1)}$, changes in firm-product level emissions can be directly attributed to shifts in firm inefficiency, as captured by $\lambda_{it}/\lambda_{i(t-1)}$:

$$\zeta_{hit}/\zeta_{hi(t-1)} = \lambda_{it}/\lambda_{i(t-1)}.$$

In contrast, when $\zeta_{ht} \neq \zeta_{h(t-1)}$, the comparison between λ_{it} and $\lambda_{i(t-1)}$ lacks a coherent interpretation.

In light of these challenges, we propose an alternative methodology, leveraging the iterative structure of our algorithm. Starting from our null hypothesis, equation (2) can be reformulated as:

$$z_{hit} = z_{it} \frac{s_{hit}\zeta_h}{\sum_{h'} s_{h'it}\zeta_{h'}}, \tag{E.1}$$

with subscript i representing a firm, rather than a firm-year observation. Equation (E.1) allocates firm-specific emissions across products, and remains valid under our assumption that $\{\zeta_{ht}\} = \{\zeta_h\}$. Subsequently, we can derive the cumulative emissions and output

Table E.1: Time Consistency of ζ_h

Emssion Type	β_1	S.E.	R^2	Rank Corr.
COD	1.00	0.00	1.00	0.96
SO_2	1.00	0.00	1.00	0.93
NOX	1.00	0.00	1.00	0.96
CO_2	1.00	0.00	1.00	0.49
Ind. Exh.	1.00	0.00	1.00	0.94
Water	1.00	0.00	1.00	0.96
Amm. Nit.	1.00	0.00	1.00	0.93
Soot	1.00	0.00	1.00	0.93
Dust	1.00	0.00	1.00	0.85

Notes: The table demonstrates a pronounced correlation between the long-run product-level emission intensities, denoted as ζ_h, and their annual fluctuations, represented by ζ'_{ht}. Displayed columns include the β_1 coefficients, accompanied by their respective standard errors and the adjusted R-squared values, all derived from estimating equation (E.3). The inclusion of year fixed effects does not alter these results. The last column displays the rank correlation between ζ_h and ζ'_{ht}.

pertinent to the product (Z_{ht} and Y_{ht}) to infer the emission intensities for year t:

$$\zeta'_{ht} = \frac{Z_{ht}}{Y_{ht}}. \tag{E.2}$$

It is noteworthy that our baseline iterative algorithm terminates once the pre-defined $\{\zeta_h\}$ (in equation (E.1)) and the right-hand side of equation (E.2) converge within an acceptable tolerance. Using this logic, the proximity between ζ_h and ζ'_{ht} can serve as a diagnostic tool, assessing the initial appropriateness of assuming ζ_h in equation (E.1).

Loosely speaking, let $\Phi_t(\cdot)$ denote the operations (E.1) and (E.2). The convergence of our algorithm at the annual level can be succinctly described as a fixed point criterion $\zeta_{ht} = \Phi_t(\zeta_{ht})$. Using our long-run average PLEI as an argument to Φ_t, we can obtain a one-step update of $\zeta'_{ht} = \Phi_t(\zeta_h)$. By observing how similar ζ'_{ht} is with ζ_h, we can get a sense of how close ζ_h is to the fixed point of $\Phi_t(\cdot)$. In the extreme case, if $\zeta_h = \zeta_{ht}$ is the fixed point of $\Phi_t(\cdot)$, we expect $\zeta'_{ht} = \zeta_h$; instead, if ζ_h is far from the fixed point (i.e., rather different from ζ_{ht}), we expect ζ'_{ht} to be quite different from ζ_h.

Upon computing ζ'_{ht}, we estimate the following equation to compare two emission intensities:

$$\ln(\zeta'_{ht}) = \beta_0 + \beta_1 \ln(\zeta_h) + \epsilon_{ht}. \tag{E.3}$$

Table E.1 presents the estimated values of β_1. Both the regression coefficients and R^2 are 1.00 for all pollutants, indicating that ζ_h captures the vast majority of the variation in ζ'_{ht}. The final column reports rank correlations generally exceeding 0.90, except in the case of CO_2. Collectively, the evidence supports a parsimonious characterization of emission intensities using their long-run averages.

F Additional Tables and Figures

Figure F.1: Cumulative Total Emissions and Trade Volume

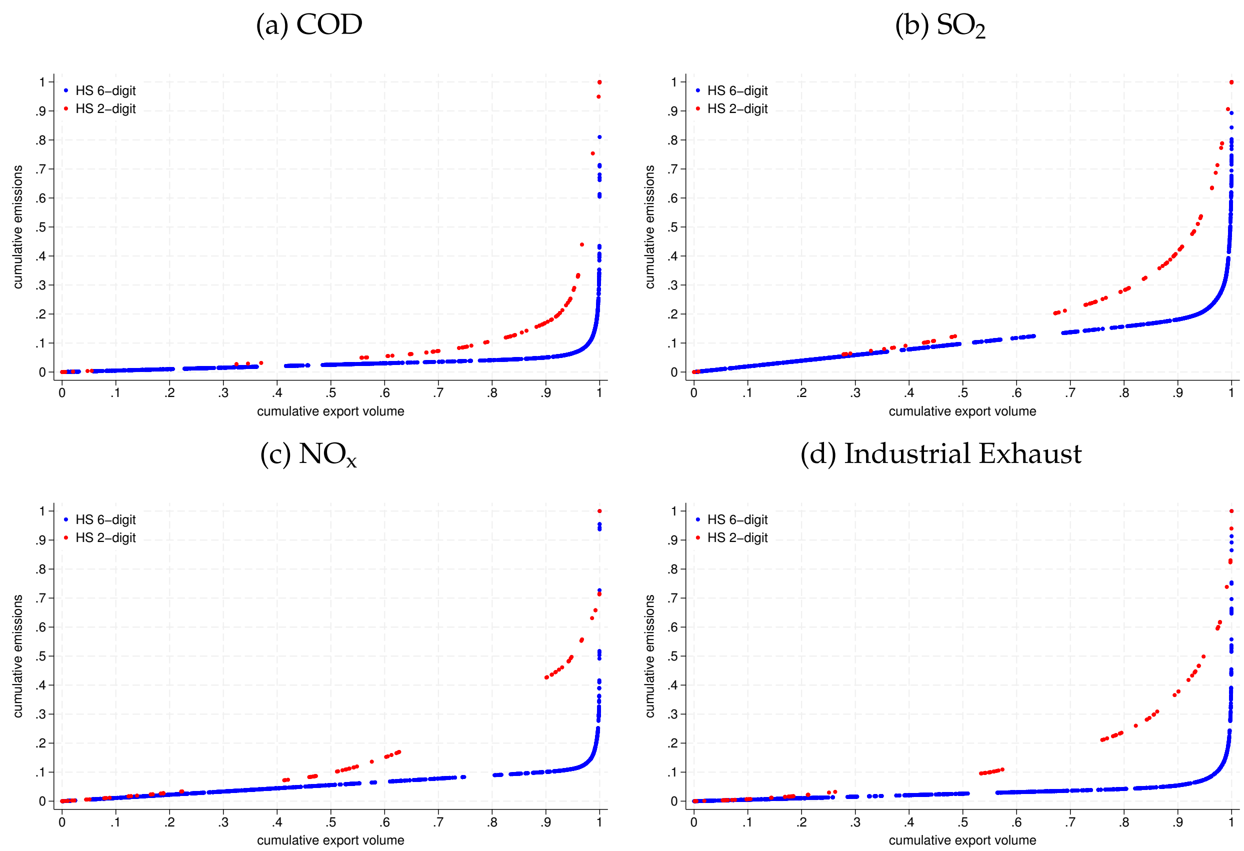

Notes: This figure illustrates the cumulative distributions of total emissions and export volumes. Products are sorted in increasing order based on their total emission intensities.

Figure F.2

(a) Water

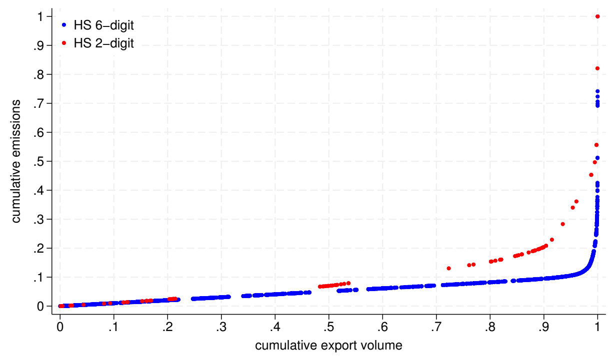

(b) Ammonical Nitrogen

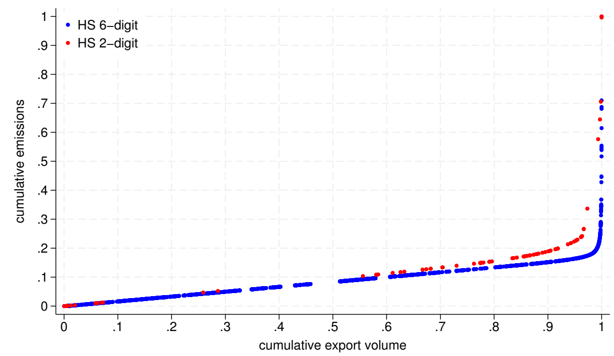

(c) Soot

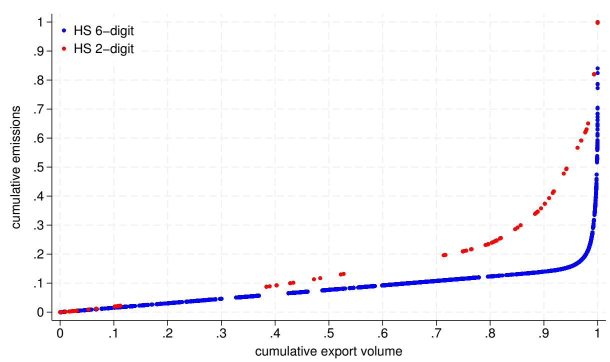

(d) Dust

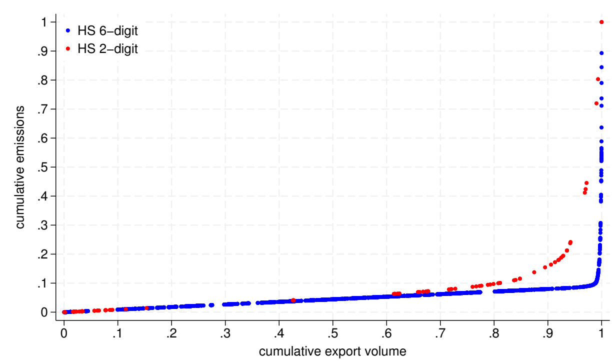

Notes: This figure illustrates the cumulative distributions of total emissions and export volumes. Products are sorted in increasing order based on their total emission intensities.

Table F.1: Top SO_2-intensive Products

HS Code	Description
810000	**Metals; n.e.c., cermets and articles thereof**
810990	Zirconium; other than unwrought, n.e.c. in heading no. 8109
811292	Gallium, germanium, hafnium, indium, niobium (columbium), rhenium and vanadium; articles ...
811299	Gallium, germanium, hafnium, indium, niobium (columbium), rhenium and vanadium; articles ...
280000	**Inorganic chemicals**
282732	Chlorides; of aluminium
283319	Sodium sulphates; other than disodium sulphate
282510	Hydrazine and hydroxylamine and their inorganic salts
710000	**Natural, cultured pearls; precious, semi-precious stones; precious metals, metals clad wi...**
710122	Pearls; cultured, worked, whether or not graded (but not strung, mounted or set), tempora...
710691	Metals; silver, unwrought, (but not powder)
711620	Stones; precious or semi-precious stones (natural, synthetic or reconstructed) articles o...
230000	**Food industries, residues and wastes thereof; prepared animal fodder**
230610	Oil-cake and other solid residues; whether or not ground or in the form of pellets, resul...
230210	Bran, sharps and other residues; of maize (corn), whether or not in the form of pellets, ...
230649	Oil-cake and other solid residues; whether or not ground or in the form of pellets, resul...
720000	**Iron and steel**
720690	Iron or non-alloy steel; primary forms (excluding ingots and iron of heading no. 7203)
721790	Iron or non-alloy steel; wire, n.e.c. in heading no. 7217
720925	Iron or non-alloy steel; (not in coils), flat-rolled, width 600mm or more, cold-rolled, o...
540000	**Man-made filaments and textile materials**
540234	Yarn, synthetic; filament, monofilament (less than 67 decitex), textured, of polypropylen...
540824	Fabrics, woven; of artificial filament yarn, containing 85% or more by weight of artific...
540831	Fabrics, woven; of artificial filament yarn, of artificial monofilament, strip and the li...

Table F.2: Top Industrial Exhaust-intensive Products

HS Code	Description
280000	**Inorganic chemicals**
282739	Chlorides; other than of ammonium, calcium, magnesium, aluminium and nickel
283911	Silicates; sodium metasilicates
283230	Thiosulphates
720000	**Iron and steel**
720825	Iron or non-alloy steel; in coils, without patterns in relief, flat-rolled, of a width 60...
720690	Iron or non-alloy steel; primary forms (excluding ingots and iron of heading no. 7203)
720719	Iron or non-alloy steel; semi-finished products of iron or non-alloy steel, containing by...
690000	**Ceramic products**
690310	Refractory ceramic goods; containing by weight more than 50% of graphite or other forms ...
690220	Refractory bricks, blocks, tiles and similar refractory ceramic constructional goods; con...
690100	Bricks, blocks, tiles and other ceramic goods of siliceous fossil meals (e.g. kieselguhr,...
250000	**Plastering materials, lime and cement**
252100	Limestone flux; limestone and other calcareous stone, of a kind used for the manufacture ...
251749	Stones; of heading no. 2515 or 2516 (excluding marble), in granules, chippings and powder...
253010	Vermiculite, perlite and chlorites; unexpanded
810000	**Metals; n.e.c., cermets and articles thereof**
810210	Molybdenum; articles thereof, including waste and scrap, powders
810390	Tantalum; articles n.e.c. in heading no. 8103
811221	Chromium and articles thereof; unwrought chromium, powders
760000	**Aluminium and articles thereof**
760521	Aluminium; alloys, wire, maximum cross-sectional dimension exceeding 7mm
760511	Aluminium; (not alloyed), wire, maximum cross-sectional dimension exceeds 7mm
760421	Aluminium; alloys, hollow profiles

Table F.3: Top Water-consuming Products

HS Code	Description
250000	**Plastering materials, lime and cement**
251749	Stones; of heading no. 2515 or 2516 (excluding marble), in granules, chippings and powder...
251741	Stones; of marble, in granules, chippings and powder, whether or not heat-treated
251320	Emery, natural corundum, natural garnet and other natural abrasives, whether or not heat-...
720000	**Iron and steel**
720825	Iron or non-alloy steel; in coils, without patterns in relief, flat-rolled, of a width 60...
721633	Iron or non-alloy steel; H sections, hot-rolled, hot-drawn or extruded, of a height of 80...
720837	Iron or non-alloy steel; in coils, without patterns in relief, flat-rolled, of a width 60...
280000	**Inorganic chemicals**
282732	Chlorides; of aluminium
281410	Ammonia; anhydrous
282710	Chlorides; of ammonium
440000	**Wood and articles of wood; wood charcoal**
440122	Wood; for fuel, in chips or particles, non-coniferous, whether or not agglomerated
441300	Wood; densified wood, in blocks, plates, strips or profile shapes
440839	Wood, tropical; as in Subheading note 2 to this Chapter, n.e.c. in item no. 4408.31, shee...
350000	**Albuminoidal substances; modified starches; glues; enzymes**
350790	Enzymes and prepared enzymes; other than rennet and concentrates thereof
350290	Albumins, albuminates and other albumin derivatives; other than egg or milk albumin, incl...
350510	Dextrins and other modified starches
290000	**Organic chemicals**
292111	Amine-function compounds; acyclic monoamines and their derivatives, methylamine, di- or t...
292243	Amino-acids, other than those containing more than one kind of oxygen function, and their...
290382	Halogenated derivatives of cyclanic, cyclenic or cycloterpenic hydrocarbons; aldrin (ISO)...

Table F.4: Top Ammoniacal Nitrogen-intensive Products

HS Code	Description
280000	**Inorganic chemicals**
283220	Sulphites; other than of sodium
282732	Chlorides; of aluminium
280530	Earth-metals, rare; scandium and yttrium, whether or not intermixed or interalloyed
810000	**Metals; n.e.c., cermets and articles thereof**
810210	Molybdenum; articles thereof, including waste and scrap, powders
810194	Tungsten (wolfram); unwrought, including bars and rods obtained simply by sintering
810294	Molybdenum; unwrought, including bars and rods obtained simply by sintering
290000	**Organic chemicals**
292411	Acyclic amides (including acyclic carbamates) and their derivatives; salts thereof; mepro...
293491	Other heterocyclic compounds, n.e.c. in 2934.1, 2934.2 and 2934.3
292424	Cyclic amides (including cyclic carbamates) and their derivatives; ethinamate and i... salts
250000	**Plastering materials, lime and cement**
251749	Stones; of heading no. 2515 or 2516 (excluding marble), in granules, chippings and powder...
250100	Salt (including table salt and denatured salt); pure sodium chloride whether or not in aq...
250850	Clays (excluding expanded clays of heading no. 6806); andalusite, kyanite and sillimanite...
50000	**Animal originated products; not elsewhere specified or included**
50210	Animal products; hair and bristles, of pigs, hogs or boars, and waste thereof
51191	Animal products; of fish or crustaceans, molluscs or other aquatic invertebrates; dead an...
50590	Animal products; skins and other parts of birds, feathers and down (not for stuffing), po...
230000	**Food industries, residues and wastes thereof; prepared animal fodder**
230250	Bran, sharps and other residues; of leguminous plants, whether or not in the form of pell...
230320	Beet-pulp, bagasse and other waste of sugar manufacture; whether or not in the form of pe...
230990	Dog or cat food; (not put up for retail sale), used in animal feeding

Table F.5: Top Soot-intensive Products

HS Code	Description
790000	**Zinc and articles thereof**
790111	Zinc; unwrought, (not alloyed), containing by weight 99.99% or more of zinc
790390	Zinc; powders and flakes
790700	Zinc; articles n.e.c. in chapter 79
310000	**Fertilizers**
310230	Fertilizers, mineral or chemical; nitrogenous, ammonium nitrate, whether or not in aqueou...
310540	Fertilizers, mineral or chemical; ammonium dihydrogenorthophosphate (monoammonium phospha...
310100	Fertilizers, animal or vegetable; whether or not mixed together or chemically treated; fe...
280000	**Inorganic chemicals**
282731	Chlorides; of magnesium
281830	Aluminium hydroxide
282510	Hydrazine and hydroxylamine and their inorganic salts
690000	**Ceramic products**
690290	Refractory bricks, blocks, tiles and similar refractory ceramic constructional goods; n.e...
690100	Bricks, blocks, tiles and other ceramic goods of siliceous fossil meals (e.g. kieselguhr,...
691110	Tableware and kitchenware; of porcelain or china
710000	**Natural, cultured pearls; precious, semi-precious stones; precious metals, metals clad wi...**
710691	Metals; silver, unwrought, (but not powder)
710122	Pearls; cultured, worked, whether or not graded (but not strung, mounted or set), tempora...
711620	Stones; precious or semi-precious stones (natural, synthetic or reconstructed) articles o...
480000	**Paper and paperboard**
480269	Uncoated paper and paperboard (not 4801 or 4803); over 10% by weight of mechanical or ch...
480421	Kraft paper and paperboard; sack kraft paper, uncoated, unbleached, in rolls or sheets, o...
481110	Paper and paperboard; tarred, bituminised or asphalted, in rolls or sheets, other than go...

Table F.6: Top Dust-intensive Products

HS Code	Description
310000	**Fertilizers**
310230	Fertilizers, mineral or chemical; nitrogenous, ammonium nitrate, whether or not in aqueou...
310430	Fertilizers, mineral or chemical; potassic, potassium sulphate
310540	Fertilizers, mineral or chemical; ammonium dihydrogenorthophosphate (monoammonium phospha...
280000	**Inorganic chemicals**
281830	Aluminium hydroxide
282919	Chlorates; other than sodium
284130	Salts; sodium dichromate
720000	**Iron and steel**
720690	Iron or non-alloy steel; primary forms (excluding ingots and iron of heading no. 7203)
721631	Iron or non-alloy steel; U sections, hot-rolled, hot-drawn or extruded, of a height of 80...
721621	Iron or non-alloy steel; L sections, hot-rolled, hot-drawn or extruded, of a height of le...
790000	**Zinc and articles thereof**
790111	Zinc; unwrought, (not alloyed), containing by weight 99.99% or more of zinc
790400	Zinc; bars, rods, profiles and wire
790390	Zinc; powders and flakes
250000	**Plastering materials, lime and cement**
253010	Vermiculite, perlite and chlorites; unexpanded
251990	Magnesia, fused or dead-burned (sintered); whether or not containing small quantities of ...
251512	Marble and travertine; merely cut, by sawing or otherwise, into blocks or slabs of a rect...
710000	**Natural, cultured pearls; precious, semi-precious stones; precious metals, metals clad wi...**
710691	Metals; silver, unwrought, (but not powder)
711590	Metal; precious or metal clad with precious metal, other than that of item no. 7115.10
710122	Pearls; cultured, worked, whether or not graded (but not strung, mounted or set), tempora...

Figure F.3: Direct vs. Total Emission Intensities

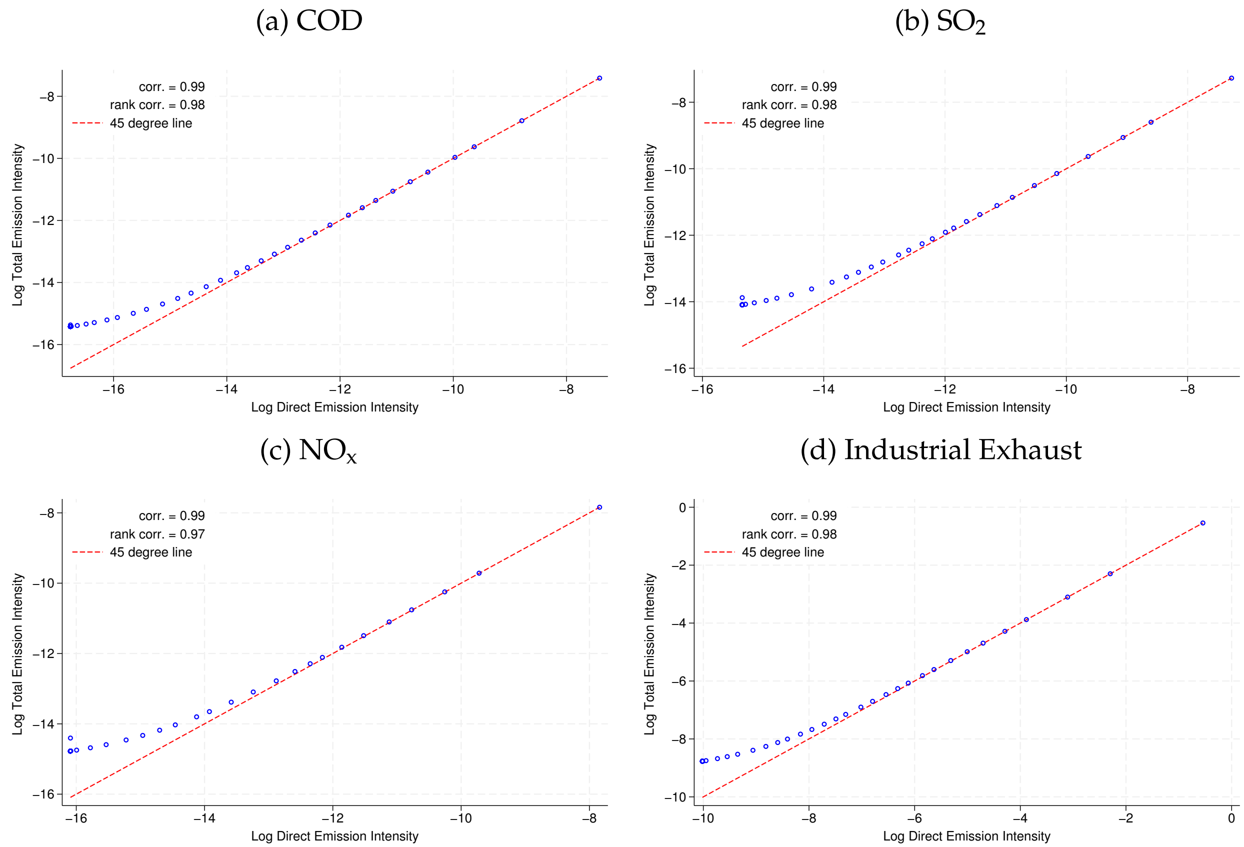

Notes: These figures compare the logarithmic values of direct and total emission intensities for various emissions. We add the smallest value of total emission intensities to all values before log transformation to account for zero emission intensities. For exposition, we sample one HS 6-digit product from each of 100 percentile values of direct emission intensities and display it as a dot. The dots presented in the figure appear to be less than 100 as many dots overlap each other toward zero direct emission intensities. The displayed correlations are derived from the full distribution of emission intensities rather than the 100 displayed dots.

Figure F.4: Direct vs. Total Emission Intensities

(a) Water Usage

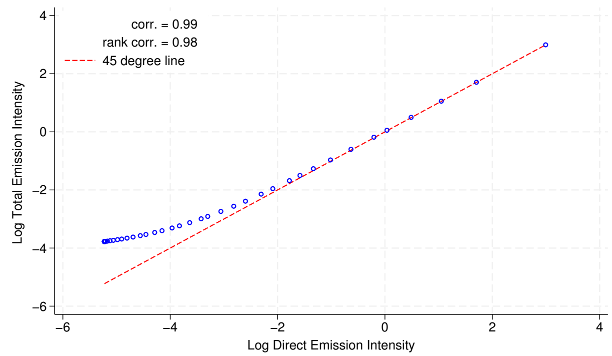

(b) Ammoniacal Nitrogen

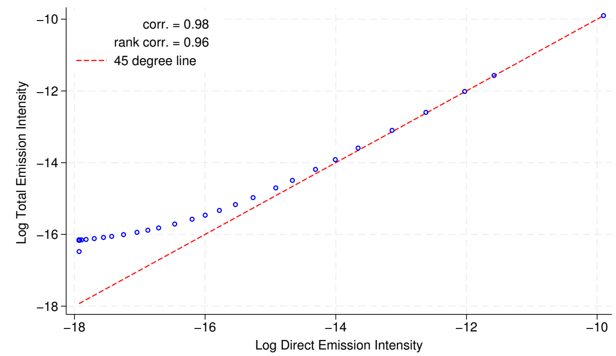

(c) Soot

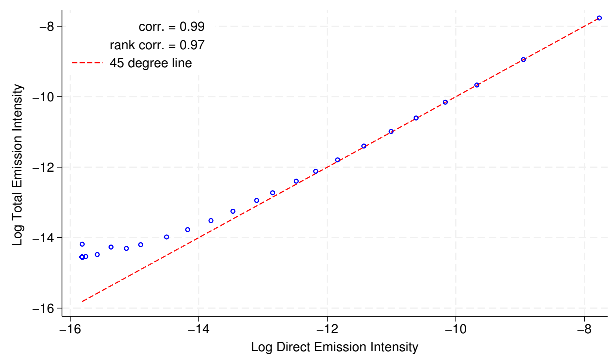

(d) Dust

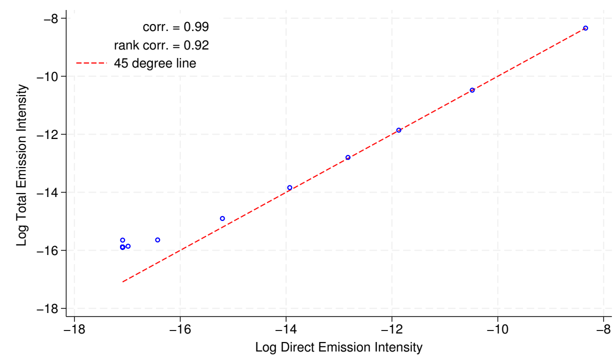

Notes: These figures compare the logarithmic values of direct and total emission intensities for various emissions. We add the smallest value of total emission intensities to all values before log transformation to account for zero emission intensities. For exposition, we sample one HS 6-digit product from each of 100 percentile values of direct emission intensities and display it as a dot. The dots presented in the figure appear to be less than 100 as many dots overlap each other toward zero direct emission intensities. The displayed correlations are derived from the full distribution of emission intensities rather than the 100 displayed dots.

Figure F.5: Distribution of λ by Productivity and Ownership

(a) By Productivity

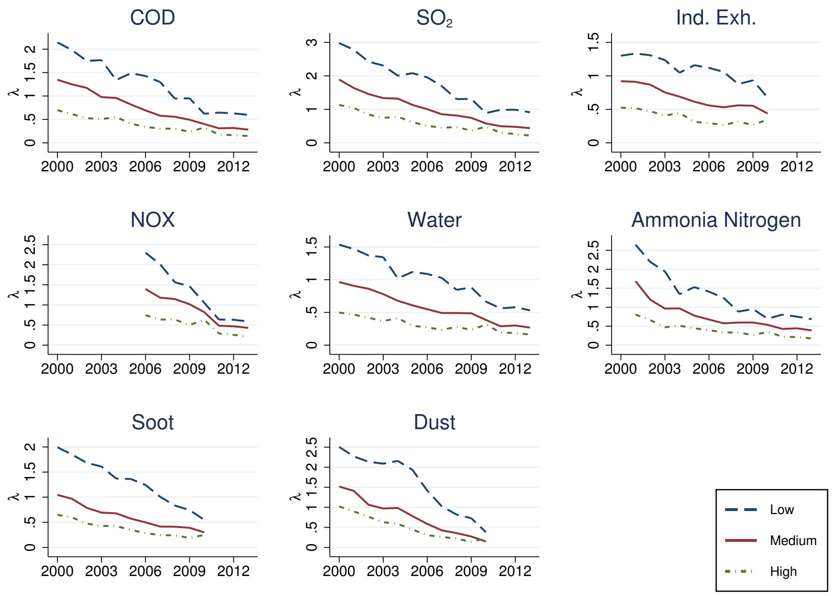

(b) By Ownership

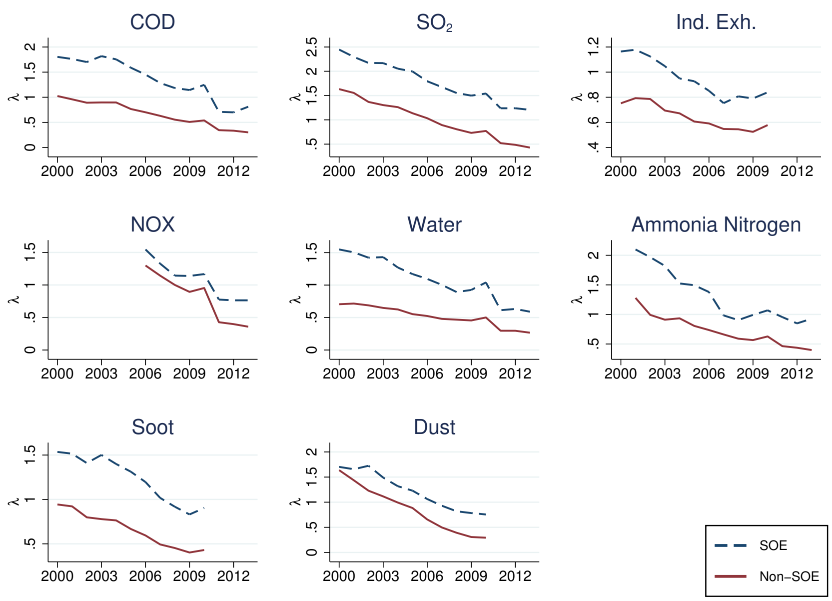

Notes: These figures show the distribution of firms' emission inefficiency parameter λ by the level of productivity (upper) and ownership (lower).

G Carbon Border Adjustment Mechanism

This appendix outlines the quantitative trade model used in the counterfactual policy analysis in Section 4.

G.1 Model

G.1.1 Utility, production and emissions

We incorporate our PLEI estimates into the European Union's Carbon Border Adjustment Mechanism (CBAM) within the quantitative trade model developed by Duan et al. (2021). The model embeds production-side emissions following Copeland and Taylor (2004), within a multi-country general equilibrium framework à la Caliendo and Parro (2015).

In each country n, a representative household maximizes utility via a Cobb-Douglas aggregator:

$$U_n = \prod_{j=1}^{J} \left(C_n^j\right)^{\beta_n^j},$$

where $\sum_{j=1}^{J} \beta_n^j = 1$, and β_n^j denotes the expenditure share on sector j.[41] Each sector j comprises a continuum of differentiated varieties $\omega^j \in [0,1]$. The composite good is given by:

$$C_n^j = \left[\int c_n^j(\omega^j)^{(\sigma_j - 1)/\sigma^j} d\omega^j\right]^{\sigma^j/(\sigma^j-1)},$$

where $\sigma^j > 0$ denotes the elasticity of substitution across varieties within sector j. The corresponding CES price index is:

$$P_n^j = \left[\int p_n^j(\omega^j)^{1-\sigma^j} d\omega^j\right]^{1/(1-\sigma^j)}.$$

The demand for variety ω^j in country n is then:

$$c_n^j(\omega^j) = \left(\frac{p_n^j(\omega^j)}{P_n^j}\right)^{-\sigma^j} Q_n^j,$$

[41] With slight abuse of notation, we use a superscript j to denote a product or sector, following standard convention in the literature.

where Q_n^j denotes total consumption of sector j.

Production of variety ω^j in country n follows:

$$y_n^j(\omega^j) = A_n^j(\omega^j) l_n^j(\omega^j)^{\gamma_{l,n}^j} \prod_{j'=1}^{J} m_n^{j'j}(\omega^j)^{\gamma_n^{j'j}},$$

where $A_n^j(\omega^j)$ denotes productivity, $l_n^j(\omega^j)$ is labor input, and $m_n^{j'j}(\omega^j)$ represents intermediate input use of product j' in the production of j. We impose $\gamma_{l,n}^j + \sum_{j'} \gamma_n^{j'j} = 1$ to ensure constant returns to scale.

Following Copeland and Taylor (2003), we assume that a fraction ϵ_n^j of gross output is allocated to abatement, yielding net output

$$q_n^j(\omega^j) = (1 - \epsilon_n^j) y_n^j(\omega^j), \tag{G.1}$$

and emissions governed by the abatement technology

$$z_n^j(\omega^j) = (1 - \epsilon_n^j)^{1/\alpha_n^j} y_n^j(\omega^j). \tag{G.2}$$

Combining (G.1) and (G.2), net output can be expressed as:

$$q_n^j(\omega^j) = \left(A_n^j(\omega^j) l_n^j(\omega^j)^{\gamma_{l,n}^j} \prod_{j'=1}^{J} m_n^{j'j}(\omega^j)^{\gamma_n^{j'j}} \right)^{1-\alpha_n^j} z_n^j(\omega^j)^{\alpha_n^j}.$$

Intermediate-good producers choose inputs to maximize profits:

$$\max_{l_n^j, m_n^{j'j}, z_n^j} p_n^j(\omega^j) q_n^j(\omega^j) - w_n l_n^j(\omega^j) - \sum_{j'=1}^{J} P_n^{j'} m_n^{j'j}(\omega^j) - t_n z_n^j(\omega^j), \tag{G.3}$$

where p_n^j denotes the output price in sector j and country n, w_n denotes the wage, $P_n^{j'}$ denotes the price of intermediate input from sector j' in country n, and t_n represents country n's shadow price of emissions. The optimized input bundle cost is:

$$\psi_n^j = \iota_{1,n}^j \, t_n^{\alpha_n^j} \, c_n^{j\,1-\alpha_n^j},$$

where c_n^j is the cost of non-emissions inputs:

$$c_n^j = \iota_{2,n}^j \,(w_n)^{\gamma_{l,n}^j} \prod_{j'=1}^{J} \left(P_n^{j'} \right)^{\gamma_n^{j'j}}.$$

The coefficients are given by:

$$\iota_{1,n}^j = (\alpha_n^j)^{-\alpha_n^j} (1 - \alpha_n^j)^{\alpha_n^j - 1}, \quad \iota_{2,n}^j = (\gamma_{l,n}^j)^{-\gamma_{l,n}^j} \prod_{j'=1}^{J} (\gamma_n^{j'j})^{-\gamma_n^{j'j}}.$$

Under perfect competition, the factory-gate price of variety ω^j is:

$$p_n^j(\omega^j) = \psi_n^j A_n^j(\omega^j)^{-(1-\alpha_n^j)}.$$

In equilibrium, the emissions intensity is:

$$\frac{z_n^j}{p_n^j q_n^j} = \frac{\alpha_n^j}{t_n}.$$

Hence, a product's emissions intensity in country n is proportional to α_n^j and inversely proportional to the carbon price t_n.

G.1.2 International trade and prices

Let $\kappa_{nn'}^j$ denote the iceberg trade cost for shipping a good in sector j from country n to country n', satisfying the triangular inequality $\kappa_{nh}^j \kappa_{hn'}^j \geq \kappa_{nn'}^j$ for any intermediary country h. Let $\tau_{nn'}^j$ denote the carbon border adjustment tax imposed by country n' on imports from country n in sector j.[42]

Under perfect competition, the price of variety ω^j available in country n is determined by the lowest-cost supplier across all potential source countries:

$$p_n^j(\omega^j) = \min_{n'} \left\{ \frac{\tau_{n'n}^j \kappa_{n'n}^j \psi_{n'}^j}{\left[A_{n'}^j(\omega^j)\right]^{1-\alpha_{n'}^j}} \right\}.$$

Following Eaton and Kortum (2002), we assume that the productivity term $\left[A_n^j(\omega^j)\right]^{1-\alpha_n^j}$ is Fréchet-distributed:

$$F^j(A) = \exp\left(-\lambda_n^j A^{-\theta^j}\right).$$

Then, the distribution of prices for goods exported from country n' to country n is:

$$\begin{aligned} G_{n'n}^j(p) = \Pr\left[p_{n'n}^j < p\right] &= \Pr\left[A_{n'}^{j(1-\alpha_{n'}^j)} > \frac{\tau_{n'n}^j \kappa_{n'n}^j \psi_{n'}^j}{p}\right] \\ &= 1 - \exp\left(-\lambda_{n'}^j \left(\frac{\tau_{n'n}^j \kappa_{n'n}^j \psi_{n'}^j}{p}\right)^{-\theta^j}\right). \end{aligned} \tag{G.4}$$

[42]The carbon border tax is allowed to be discriminatory. The consistency of such measures with the nondiscrimination principle under the General Agreement on Tariffs and Trade (GATT) is debated. If carbon content varies substantially across countries, a discriminatory ad valorem tax may, in effect, be nondiscriminatory.

The cumulative distribution of prices available to country n is then:

$$G_n^j(p) = \Pr(P_n^j < p) = 1 - \prod_{n'=1}^{N} \left[1 - G_{n'n}^j(p)\right] = 1 - \exp\left(-\Phi_n^j p^{\theta^j}\right), \tag{G.5}$$

where the price competitiveness index Φ_n^j is defined as:

$$\Phi_n^j \equiv \sum_{n'=1}^{N} \lambda_{n'}^j \left(\tau_{n'n}^j \kappa_{n'n}^j \psi_{n'}^j\right)^{-\theta^j}.$$

The sectoral price index in country n is given by:

$$\begin{aligned}
\left(P_n^j\right)^{1-\sigma^j} &= \int_0^\infty p^{1-\sigma^j}\, dG_n^j(p) && \text{(G.6)}\\
&= \left(\Phi_n^j\right)^{-\frac{1-\sigma^j}{\theta^j}} \int_0^\infty \left(\Phi_n^j p^{\theta^j}\right)^{\frac{1-\sigma^j}{\theta^j}} \exp\left(-\Phi_n^j p^{\theta^j}\right) d\left(\Phi_n^j p^{\theta^j}\right) && \text{(G.7)}\\
&= \left(\Phi_n^j\right)^{-\frac{1-\sigma^j}{\theta^j}} \Gamma\left(\frac{\theta^j + 1 - \sigma^j}{\theta^j}\right). && \text{(G.8)}
\end{aligned}$$

Rearranging yields:

$$P_n^j = \iota_3^j \left[\sum_{n'=1}^{N} \lambda_{n'}^j \left(\tau_{n'n}^j \kappa_{n'n}^j \psi_{n'}^j\right)^{-\theta^j}\right]^{-\frac{1}{\theta^j}},$$

where

$$\iota_3^j \equiv \left[\Gamma\left(1 + \frac{1-\sigma^j}{\theta^j}\right)\right]^{\frac{1}{1-\sigma^j}}$$

is a constant, defined provided that $\theta^j > \sigma^j - 1$. Given Cobb-Douglas preferences, the aggregate price index in country n is:

$$P_n = \prod_{j=1}^{J} \left(\frac{P_n^j}{\beta_n^j}\right)^{\beta_n^j}.$$

Let X_n^j denote total expenditure on good j in country n, encompassing both final and intermediate demand. The share of this expenditure spent on imports from country n' is denoted by $\pi_{n'n}^j$, where:

$$\pi_{n'n}^j = \frac{X_{n'n}^j \tau_{n'n}^j}{X_n^j},$$

and $X_{n'n}^j$ denotes the pre-tax value of exports from n' to n. Under the model assumptions, we derive the trade share expression:

$$\pi_{n'n}^j = \frac{\lambda_{n'}^j \left(\tau_{n'n}^j \kappa_{n'n}^j \psi_{n'}^j\right)^{-\theta^j}}{\Phi_n^j}.$$

G.1.3 Market Clearing and Trade Balance

Total expenditure on good j in country n consists of intermediate input demand from firms and final consumption by households, following Caliendo and Parro (2015).

$$X_n^j = \sum_{j'=1}^{J}(1-\alpha_n^{j'})\gamma_n^{j,j'}\sum_{n'=1}^{N}\frac{\pi_{nn'}^{j'}X_{n'}^{j'}}{\tau_{nn'}^{j}} + \beta_n^j I_n.$$

Let T_n^j denote domestic emission tax revenue in sector j of country n:

$$T_n^j = t_n z_n^j.$$

Aggregating across all sectors, total domestic carbon tax revenue is:

$$T_n = \sum_{j=1}^{J} T_n^j.$$

Under the Cobb-Douglas structure, this simplifies to:

$$T_n = \sum_{j=1}^{J}\sum_{n'=1}^{N}\frac{\alpha_n^j \pi_{nn'}^j X_{n'}^j}{\tau_{nn'}^j}.$$

Let $T_{n'n}^{Bj}$ denote carbon border tax revenue collected by country n on imports from country n' in sector j:[43]

$$T_{n'n}^{Bj} = X_{n'n}^j\left(\tau_{n'n}^j - 1\right).$$

Total carbon border tax revenue for country n is then:

$$T_n^B = \sum_{n'}\sum_{j} T_{n'n}^{Bj}.$$

We denote the national trade deficit by $D_n = \sum_{j=1}^{J} D_n^j$. Accordingly, household income in country n is:

$$I_n = w_n L_n + T_n + T_n^B + D_n. \tag{G.9}$$

The equilibrium wage rate w_n is determined by the labor market clearing condition:

$$w_n L_n = \sum_{j=1}^{J}\gamma_{l,n}^j(1-\alpha_n^j)\sum_{n'=1}^{N}\frac{\pi_{nn'}^j X_{n'}^j}{\tau_{nn'}^j}. \tag{G.10}$$

Substituting the labor market clearing condition and the household budget constraint into

[43] In our counterfactual analysis, effective tariffs include the prevailing tariffs and additional tariffs due to the CBAM. Thus, $T_{n'n}^{Bj}$ include the tariff revenue due to existing tariffs and additional proceeds from implementing the CBAM.

the expression for total expenditure yields the trade balance condition:

$$\sum_{j=1}^{J}\sum_{n'=1}^{N}\frac{X_n^j\pi_{n'n}^j}{\tau_{n'n}^j}-D_n=\sum_{j=1}^{J}\sum_{n'=1}^{N}\frac{X_{n'}^j\pi_{nn'}^j}{\tau_{nn'}^j}, \tag{G.11}$$

where the left-hand side represents total absorption in country n across all sectors, and the right-hand side captures the value of goods produced by country n and sold abroad. A positive trade deficit, $D_n > 0$, indicates that country n absorbs more than it produces, reflecting excess demand relative to output.

G.1.4 Exact hat algebra

Following Dekle et al. (2008), Caliendo and Parro (2015), and Duan et al. (2021), we express the model's equilibrium in changes using exact-hat algebra, which facilitates counterfactual policy analysis without requiring the calibration of unobserved levels of trade costs, productivity, or prices.

Definition 1. *Let $\{w_n, P_n^j\}_{j=1,n=1}^{J,N}$ and $\left\{(w_n)', (P_n^j)'\right\}_{j=1,n=1}^{J,N}$ denote the equilibrium wage and price levels before and after a counterfactual change. We define the relative equilibrium response $\left\{\hat{w}_n, \hat{P}_n^j\right\}_{j=1,n=1}^{J,N}$ to a policy shock – such as changes in domestic carbon taxes, productivity, or carbon border taxes – denoted by $\left\{\hat{t}_n, \hat{\lambda}_n^j, \hat{\tau}_{nn'}^j\right\}$. These relative changes must satisfy the following equilibrium conditions:*

Cost of production:

$$\hat{\psi}_n^j = \left(\hat{t}_n^j\right)^{\alpha_n^j}\left[(\hat{w}_n)^{\gamma_{l,n}^j}\prod_{j'=1}^{J}\left(\hat{P}_n^{j'}\right)^{\gamma_n^{j'j}}\right]^{1-\alpha_n^j};$$

Sectoral price index:

$$\hat{P}_n^j = \left[\sum_{n'=1}^{N}\pi_{n'n}^j\hat{\lambda}_{n'}^j\left(\hat{\tau}_{n'n}^j\hat{\psi}_{n'}^j\right)^{-\theta^j}\right]^{-1/\theta^j};$$

Bilateral trade shares:

$$\hat{\pi}_{n'n}^j = \hat{\lambda}_{n'}^j\left(\frac{\hat{\tau}_{n'n}^j\hat{\psi}_{n'}^j}{\hat{P}_n^j}\right)^{-\theta^j};$$

Total expenditures in the counterfactual:

$$\left(X_n^j\right)' = \sum_{j'=1}^{J} \left(1 - \alpha_n^{j'}\right) \gamma_n^{jj'} \sum_{n'=1}^{N} \frac{\left(\pi_{nn'}^{j'}\right)'}{\left(\tau_{nn'}^{j'}\right)'} X_{n'}^{j'} + \beta_n^j I_n';$$

Labor market clearing:

$$\hat{w}_n w_n L_n = \sum_{j=1}^{J} \gamma_{l,n}^j \left(1 - \alpha_n^j\right) \sum_{n'=1}^{N} \frac{\left(\pi_{nn'}^j\right)'}{\left(\tau_{nn'}^j\right)'} \left(X_{n'}^j\right)';$$

where income in the new equilibrium is

$$I_n' = \hat{w}_n w_n L_n + \sum_{j=1}^{J} \sum_{n'=1}^{N} \alpha_n^j \frac{\left(\pi_{nn'}^j\right)'}{\left(\tau_{nn'}^j\right)'} \left(X_{n'}^j\right)' + \sum_{j=1}^{J} \sum_{n'=1}^{N} \left[\left(\tau_{n'n}^j\right)' - 1\right] \frac{\left(\pi_{n'n}^j\right)'}{\left(\tau_{n'n}^j\right)'} \left(X_n^j\right)' + D_n'.$$

Counterfactual f.o.b. trade flows:

$$\left(X_{nn'}^j\right)' = \frac{\left(\pi_{n'n}^j\right)'}{\left(\tau_{n'n}^j\right)'} \left(X_n^j\right)';$$

Trade balance:

$$\sum_{j=1}^{J} \sum_{n'=1}^{N} \frac{\left(\pi_{n'n}^j\right)'}{\left(\tau_{n'n}^j\right)'} \left(X_n^j\right)' - D_n' = \sum_{j=1}^{J} \sum_{n'=1}^{N} \frac{\left(\pi_{nn'}^j\right)'}{\left(\tau_{nn'}^j\right)'} \left(X_{n'}^j\right)'.$$

G.2 Data

To operationalize the counterfactual CBAM simulations at both the sector and product levels, we incorporate additional data sources. Specifically, we use the World Input-Output Database (WIOD) (Timmer et al., 2015) to obtain the input-output structure for all countries in the analysis. We aggregate the 34 non-tradeable WIOD sectors into 10 consolidated non-tradeable sectors for tractability.[44] The 21 tradable WIOD sectors are matched

[44] Industrial and Manufacturing (Repair and installation of machinery and equipment, Electricity, gas, steam and air conditioning supply); Environmental and Construction Services (Water collection, treatment, and supply, Sewerage; waste collection, treatment and disposal activities; materials recovery; remediation activities and other waste management services, Construction); Trade and Repair Services (Wholesale and retail trade and repair of motor vehicles and motorcycles, Wholesale trade, except of motor vehicles and motorcycles, Retail trade, except of motor vehicles and motorcycles); Transportation and Logistics (Land transport and transport via pipelines, Water transport, Air transport, Warehousing and support activities for transportation, Postal and courier activities); Hospitality and Food Services (Accommodation and food service activities); Media and Telecommunications (Publishing activities, Motion picture, video and television programme production, sound recording and music publishing activities; programming and broadcasting activities, Telecommunications, Computer programming, consultancy and related activities; information service activities); Financial and Insurance Services (Financial service activities, except insurance and pension funding, Insurance, reinsurance and pension funding, except compulsory social security, Activities auxiliary to financial services and insurance activities); Real Estate and Professional Services (Real

to HS 6-digit codes using the GPT-4o model API, based on detailed product and sector descriptions. One tradable sector - Forestry and Logging - is excluded from the analysis, as it cannot be reliably mapped to any HS 6-digit products.

Using the WIOD, we obtain data on intermediate input shares $\gamma_n^{j',j}$, value-added shares $\gamma_{l,n}^j$, and final demand shares β_n^j for each country-sector pair. The WIOD environmental accounts provide country-sector-level CO_2 emission intensities, which we use to infer emission elasticities α_n^j, as described below. We also extract country-level value added (in USD) and country-sector expenditure data X_n^j from WIOD.

Trade elasticities at the HS 6-digit level are taken from Fontagné et al. (2022). Sectoral trade elasticities are computed as the median elasticity across all products mapped to each sector. Trade deficits at the country level are calculated using the BACI database (Gaulier and Zignago, 2010). Throughout our counterfactual analysis, we hold trade deficits constant at their baseline levels. Tariff data at the HS 6-digit level are obtained from CEPII - MAcMap-HS6 (Guimbard et al., 2012).

Country-level carbon taxes t_n are calibrated from the identity $t_n = \alpha_n/\zeta_n$, where ζ_n is the country-level emission intensity. Following Duan et al. (2021), we infer sector- and product-level emission elasticities α_n^j by imposing the ratio $\alpha_n^j/\alpha_n^{j'} = \zeta_n^j/\zeta_n^{j'}$ and scaling to match the national average elasticity.[45]

As in Duan et al. (2021), we adopt the national emission intensity estimate for the United States, $\hat{\alpha}_{US}^{SW} = 0.011$, with the superscript SW referencing the estimates from

estate activities, Legal and accounting activities; activities of head offices; management consultancy activities, Architectural and engineering activities; technical testing and analysis, Scientific research and development, Advertising and market research, Other professional, scientific and technical activities; veterinary activities); Public Services and Education (Administrative and support service activities, Public administration and defence; compulsory social security, Education); Health, Social Work, and Other Services (Human health and social work activities, Other service activities, Activities of households as employers; undifferentiated goods- and services-producing activities of households for own use, Activities of extraterritorial organizations and bodies)

[45]Some Chinese products exhibit exceptionally high emission intensities, leading to values of product-level emission elasticities exceeding one. To address this, we scale down China's sectoral and product-level emission elasticities by a factor of 50. While this adjustment affects the absolute level of emission intensities in the model, it does not impact our counterfactual results, which are based on percentage changes in emissions.

Shapiro and Walker (2018). To extend this calibration across countries, we estimate the following cross-country regression:

$$\ln Q_n = \beta_0 + \beta_1 \ln EPS_n + \beta_2 \ln \zeta_n + \epsilon_n, \tag{G.12}$$

where Q_n is the OECD's environment-related tax revenue as a share of GDP, EPS_n denotes the OECD's Environmental Policy Stringency Index (Botta and Koźluk, 2014), and ζ_n is the country-level emission intensity.

However, the EPS index is available only for OECD countries and a subset of major developing economies (including Brazil, Russia, India, China, and South Africa). As a result, four countries in our sample – Bulgaria, Lithuania, Latvia, and Romania – lack direct EPS coverage. To address this, we draw on the Environmental Regulatory Regimes Index (ERRI) from Esty and Porter (2001), reported in the 2000–2001 Global Competitiveness Report. Although ERRI is only available for a single cross-section (the year 2000), we estimate a univariate regression of the EPS index on ERRI for countries where both measures are available. We then impute the missing EPS values, $\hat{\text{EPS}}$, for these four countries using the fitted regression.

The identification assumption underlying equation (G.12) is that α_n (emission elasticity) and Q_n share the same partial elasticities with respect to EPS_n and ζ_n. This assumption is justified, as environment-related tax revenue as share of GDP is equivalent to the output elasticity of emissions at the aggregate level.

Using equation (G.12), we estimate $\hat{\beta}_1$ and $\hat{\beta}_2$, and set the intercept C so that $\ln \hat{\alpha}_{US}^{SW} = C + \hat{\beta}_1 \ln EPS_{US} + \hat{\beta}_2 \ln \zeta_{US}$. Based on the resulting parameters and each country's EPS_n and ζ_n, we recover $\hat{\alpha}_n$ as

$$\hat{\alpha}_n = \hat{\alpha}_{US}^{SW} \left(\frac{EPS_n}{EPS_{US}} \right)^{\hat{\beta}_1} \left(\frac{\zeta_n}{\zeta_{US}} \right)^{\hat{\beta}_2}.$$

To impute country-product level emission elasticities, we exploit the proportionality $\alpha_n^j / \alpha_n^{j'} = \zeta_n^j / \zeta_n^{j'}$ to generate the cross-sectional distribution of $\hat{\alpha}_n^j$ within each country. The arithmetic mean is governed to match the national average, $\sum_j \alpha_n^j / J = \alpha_n$, where J denotes the number of products.

G.3 Regional and Product Aggregation

The full-scale quantitative trade model comprises 38 countries, 4,468 tradable products, and 34 non-tradable sectors—an intractable dimensionality for computation. To address this, we aggregate both regions and products while preserving PLEI heterogeneity. As discussed in Section G.2, the 34 non-tradable WIOD sectors are consolidated into 10 non-tradable sectors. The 4,468 tradable products are mapped to 21 tradable WIOD sectors. Within each tradable sector, we aggregate all clean products ($\alpha = 0$) into a representative clean product for that sector, while dirty products ($\alpha > 0$) are kept distinct.

For regional aggregation, we treat all EU countries as a single region, and group all countries other than China and the EU as "Rest of the World" (RoW). After aggregation, the model consists of 3 regions (China, EU, RoW), 1,134 dirty tradable products, 21 representative clean tradable products, and 10 non-tradable sectors.

To aggregate the 38-country model to three regions, we consolidate the relevant parameters using either country total output shares or country-sector output shares as weights. Specifically, emission elasticities α_n^j, input shares γ_n^j, final demand shares β_n^j, and bilateral export shares $\pi_{nn'}^j$ are aggregated using country-sector output shares. The domestic carbon tax t_n is weighted by each country's total output share. Figure G.1 compares sector-level CBAM results under the 38-country and 3-region models. The 3-region simulation slightly under-predicts emission reductions compared to the full model, but the quantitative results are broadly comparable.

Figure G.1: Effect of Sector-Level CBAM on Trade and Emissions (38 Countries vs. 3 Regions)

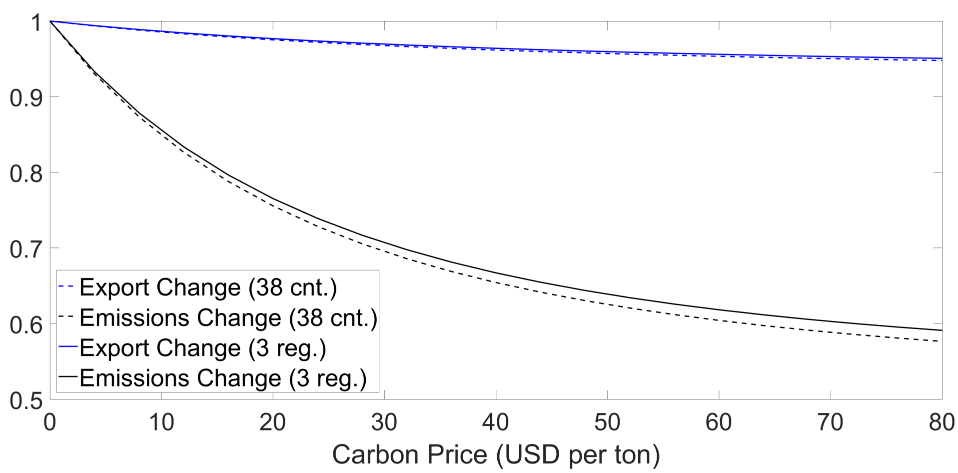

Notes: The figure compares the total change in China-to-EU exports and emissions under different carbon prices. Dashed lines represent simulations using a 38-country model; solid lines use a 3-region aggregation.